Exploring Activated Carbons for Sustainable Biogas Upgrading: A Comprehensive Review

Deneb Peredo-Mancilla, Alfredo Bermúdez, Cécile Hort, David Bessières

energies

MDPI

Review

Exploring Activated Carbons for Sustainable Biogas Upgrading: A Comprehensive Review

Deneb Peredo-Mancilla [1], Alfredo Bermúdez [1], Cécile Hort [2] and David Bessières [3,*]

[1] Department of Fisheries Engineering, Autonomous University of Baja California Sur, La Paz 23080, Mexico; dperedo@uabcs.mx (D.P.-M.); abermudez@uabcs.mx (A.B.)
[2] Laboratoire de Thermique, Energetique et Procedes-IPRA, EA1932, Université Pau, Pays Adour/E2S UPPA, 64000 Pau, France; cecile.hort@univ-pau.fr
[3] Laboratoire des Fluides Complexes et Leurs Reservoirs-IPRA, UMRS5150, Université Pau, Pays Adour/E2S UPPA, 64000 Pau, France
* Correspondence: david.bessieres@univ-pau.fr

Abstract

Global energy supply remains, to this day, mainly dominated by fossil fuels, aggravating climate change. To increase and diversify the share of renewable energy sources, there is an urgent need to expand the use of biofuels that could help in decarbonizing the energy mix. Biomethane, obtained by upgrading biogas, simultaneously allows the local production of clean energy, waste valorization, and greenhouse gas emissions mitigation. Among various upgrading technologies, the use of activated carbons in adsorption-based separation systems has attracted significant attention due to their versatility, cost-effectiveness, and sustainability potential. The present review offers a comprehensive analysis of the factors that influence the efficiency of activated carbons on carbon dioxide adsorption and separation for biogas upgrading. The influence of activation methods, activation conditions, and precursors on the biogas adsorption performance of activated carbons is revised. Additionally, the role of adsorbent textural and chemical properties on gas adsorption behavior is highlighted. By synthesizing current knowledge and perspectives, this work provides guidance for future research that could help in developing more efficient, cost-effective, and sustainable adsorbents for biogas upgrading.

Keywords: activated carbons; biogas; adsorption; upgrading

Academic Editor: Prasad Kaparaju

Received: 7 May 2025
Revised: 4 July 2025
Accepted: 8 July 2025
Published: 28 July 2025

Citation: Peredo-Mancilla, D.; Bermúdez, A.; Hort, C.; Bessières, D. Exploring Activated Carbons for Sustainable Biogas Upgrading: A Comprehensive Review. *Energies* **2025**, *18*, 4010. https://doi.org/10.3390/en18154010

1. Introduction

In the race to meet the United Nations (UN) 2030 Agenda and its Sustainable Development Goals [1], there is an urgent need for alternative energy sources and technologies that can help signatory countries "increase substantially the share of renewable energy in the global energy mix" by 2030 (Goal 7, Target 7.2). Progress on this target could also positively impact other key objectives—for example, achieving universal access to affordable, modern energy services (Target 7.1) and reducing annual national greenhouse gas emissions (Indicator 13.2.2). Moreover, since access to clean energy underpins the achievement of many other goals, special attention must be paid to Goal 7. In this context, the International Energy Agency (IEA) forecasts an overall increase in approximately 60% in renewable energy consumption (including electricity, heat, and transport) by 2030, raising the share of renewables in final energy use from 13% in 2023 to nearly 20%. Renewable biofuels, hydrogen, and e-fuels are expected to contribute around 15% of that increase [2].

In particular, biogas production from various organic waste streams—such as municipal solid waste, wastewater, agricultural residues, livestock manure, fish farms, and food waste—simultaneously reduces greenhouse gas emissions in two ways: by replacing conventional energy sources and by avoiding emissions from the natural decomposition of organic matter. In addition to these climate benefits, biogas production offers a long list of co-benefits, including improved waste management, support for circular economy strategies, enhanced energy security, availability of a versatile local energy source, provision of clean cooking fuel, and synergies with agricultural systems [3,4]. It is therefore not surprising that global demand for biogases is expected to increase by 30% between 2024 and 2030 [2], helping to decarbonize energy systems where other renewable sources face technological or availability limitations, while also contributing to reductions in global methane emissions.

While the exact composition of biogas varies among authors, it is well established that its two main components are methane (40–80% *v*/*v*) and carbon dioxide (20–55% *v*/*v*). In addition to these, biogas may also contain other components in smaller proportions, including hydrogen sulfide, water vapor, nitrogen, oxygen, volatile organic compounds, ammonia, carbon monoxide, hydrocarbons, hydrogen, particulate matter, halogenated compounds, volatile siloxanes, and other trace gases. The specific composition depends on several factors, such as the type of feedstock, the anaerobic digestion process, and the operational conditions of the system [3,5–10].

In order to improve the usability of biogas, it must be upgraded to biomethane through the removal of carbon dioxide and other impurities. This process increases its heating value and energy density from approximately 21–24 MJ/m^3 (raw biogas) to approximately 36 MJ/m^3 (biomethane) [9,11]; enhances its applicability as a substitute for natural gas in sectors such as transport, industry, power generation, and heating, thus providing lower-carbon energy options for multiple sectors; ensures compatibility with existing natural gas infrastructure; and facilitates renewable energy integration. It also eliminates harmful components and can lead to economic benefits. Some studies also highlight that the high-purity CO_2 stream obtained during upgrading could be captured and permanently stored or reused in long-living products, contributing to carbon dioxide removal strategies [12]. In effect, biogas upgrading transforms a gas with limited applications into a versatile, high-value fuel that could help in climate change mitigation and even result in net negative greenhouse gas emissions when coupled with CO_2 capture and storage [13–18].

Several upgrading technologies are commercially available. Among adsorption-based methods, Pressure Swing Adsorption (PSA) and Vacuum Swing Adsorption (VSA) are the most established, typically using activated carbon or zeolite materials such as SAPO-34 and LTA [19–21]. Other commercial approaches include Water Scrubbing (WS) [22–24], Amine Scrubbing [25–27], Membrane Separation [28–30], and Cryogenic Separation [31–33].

Emerging technologies focus on increasing selectivity, lowering energy use, or enabling circularity. These include electrochemical CO_2 separation [8,34,35], biological upgrading processes such as hydrogenotrophic methanation [36,37] and algal biofixation [38,39], hydrate-based separation [40,41], and inorganic solvent scrubbing using alkaline solutions [42,43].

The selection of a biogas upgrading strategy depends on a combination of factors, including biogas composition, target biomethane quality, economic and environmental considerations, scalability, and material availability [7,8,10,44,45]. Current trends emphasize decentralized, small-scale upgrading systems; the integration of upgrading into biorefineries; and alignment with policy drivers [7]. Novel approaches and materials

continue to emerge, particularly for low-cost, modular applications based on waste-derived adsorbents [46–48].

In particular, adsorption-based methods are widely regarded as among the most versatile and effective technologies for biogas upgrading [49]. Among these, Pressure Swing Adsorption (PSA) has been particularly established for CH_4/CO_2 separation [8]. The main advantages of this technology are the lack of chemical issues and its dry nature, which eliminates the concern of contaminated wastewater (amine and water scrubbing) [45].

Adsorbents play a critical role in CH_4/CO_2 separation. The choice of the adsorbent material is key for the optimization of a Pressure Swing Adsorption plant, as well as for other adsorption-based gas separation industrial applications such as Carbon Capture and Storage (CCS) [50], Adsorbed Natural Gas (ANG) [51], and hydrogen purification [52]. To achieve effective separation, an adsorbent must exhibit high selectivity, which depends on carefully designed properties [15,49,53,54]. Key characteristics include pore structure, surface chemistry, and interaction affinity with CO_2 molecules [49,55–61]. For instance, Gao et al. emphasize the importance of pore size distribution in enhancing CO_2 selectivity in carbon-based adsorbents [62].

In this context, material development plays a crucial role in adsorption-based upgrading. A wide range of adsorbents have been investigated for biogas upgrading systems, including carbonaceous materials such as activated carbons and Carbon Molecular Sieves with particular emphasis on biomass-derived adsorbents [63–65], zeolites [66,67], and metal–organic frameworks (MOFs) [68,69]. These materials aim to improve CO_2 selectivity, lower regeneration costs, and align with sustainability goals.

Activated carbons have attracted significant interest due to their developed porous structure, efficiency, adaptability, and relatively low cost, even more so when produced using renewable biomass as a source. Its performance can be further improved through surface modification and functionalization [50,70,71]. Emerging carbonaceous materials include modified activated carbons and biomass-derived adsorbents, each aiming to enhance selectivity, reduce cost, and improve scalability [49].

This review aims to provide a comprehensive and critical overview of current and emerging carbonaceous adsorbents for CH_4/CO_2 separation in the context of biogas upgrading. Building on the growing recognition of biogas as a key contributor to renewable energy systems and carbon mitigation strategies, the paper focuses on adsorption-based technologies, with an emphasis on the role, performance, and development potential of activated carbons. The review also highlights recent advances in material design strategies aiming to improve the adsorption behavior of these adsorbents for the optimization of biogas upgrading. This work intends to support future research efforts and inform material selection and process design for more efficient and climate-relevant biogas upgrading systems. In doing so, this review provides guidance for future research and innovation around cost-effective, climate-relevant upgrading materials, processes, and strategies.

2. Carbonaceous Adsorbents for Biogas Upgrading

Carbon-based adsorbent materials have general properties, such as high thermal and chemical stabilities, that make them suitable materials for different gas adsorption and storage applications [72], high specific surface area [52], large pore volumes, and tunable surface chemistry [73]. In addition, the required energy for the adsorption/desorption phases is low since they can be regenerated usually with temperatures lower than 373 K, and can work at atmospheric pressure [74]. Carbonaceous adsorbents include crystalline arrangements (allotropic carbon forms) such as graphite, graphene, and carbon nanotubes (CNT) or short-range ordered carbon atoms without a crystalline structure (amorphous forms), including Carbon Molecular Sieves (CMS) and Activated Carbons (AC).

In particular, understanding and optimizing the adsorption properties of activated carbons has attracted a lot of research in recent years. This type of adsorbent is known for having commendable textural and physicochemical properties, including high surface area (>1000 $m^2 g^{-1}$), tunable porosity, cycling stability, and low energy desorption requirements [75]. Their adsorption mechanism is based on equilibrium conditions, i.e., the amount of adsorbate equals the amount desorbed, resulting in their ability to retain adsorption over long periods of time, making them suitable for long-term storage and removal applications. They can be produced from a variety of different raw materials such as biomass, coal, wood, and polymers, which makes them an affordable alternative. These characteristics have resulted in ACs being widely used for several industrial and commercial adsorption applications, including wastewater treatment [76–79], food industry [80,81], capacitors [82–85], and gas storage and purification.

2.1. Activated Carbon Carbon Dioxide Adsorption Mechanism

Carbon dioxide adsorption by activated carbons is carried out by a physisorption process mainly based on weak intermolecular forces known as van der Waals forces, as indicated by low adsorption enthalpies $\Delta H° < 20$ kJ/mol (chemical adsorption $\Delta H°$ values are within 80–200 kJ/mol) [86]. The forces behind the physisorption process are explained by temporary fluctuations in the electronic distribution around molecules, which results in instantaneous dipole moments [87]. When carbon dioxide molecules are in close vicinity to the surface of activated carbons, the pi electrons of the C-O bonds in CO_2 interact with the unhybridized orbitals of carbon surface atoms, resulting in dipole-induced quadrupole short-range attraction forces as schematized in Figure 1 [88]. Methane molecules are also attracted due to London Forces; however, the quadrupole moment of CO_2 results in preferential adsorption over the non-polar CH_4 molecules.

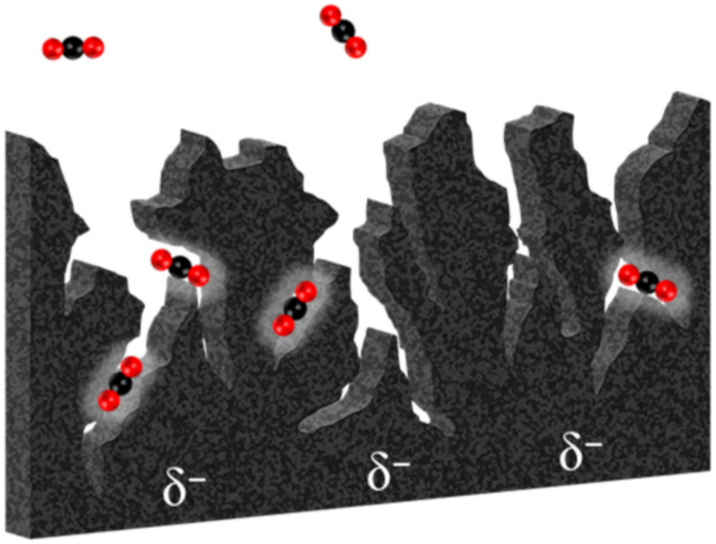

Figure 1. Schematic illustrations of CO_2 adsorption mechanism on activated carbon (source: [88]).

London forces are highly sensitive to the distance between the adsorbate molecules and the adsorbent surface groups. They are considered to be negligible at distances greater than two molecular layers, and thus the adsorption of carbon dioxide molecules happens in pores within the carbon structure, not greater than four or five molecular layers [89].

Activated carbons are prepared by a two-step method: First, a heat treatment, which raises the specific surface area, and, second, a physical or chemical activation in which porosity is developed and opened [20]. The resulting material is highly porous with a wide range of pore sizes (see Figure 2), with larger pores acting as transport pores,

allowing the diffusion of the adsorbate molecules into the adsorption sites in the smaller pores (micropores) in which the gap between the layers of carbon plates are small enough for sufficient intermolecular forces for adsorption to occur. The diffusion into smaller pores is governed by pressure gradients between the outside of the carbonaceous material and the inside of the pores.

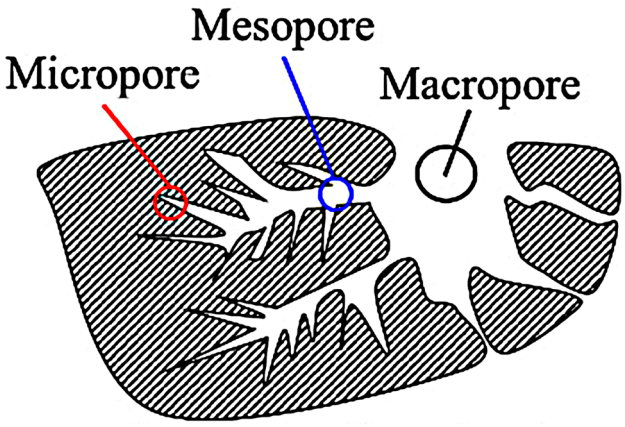

Figure 2. Schematic pore structure of activated carbons (Source: [90]).

The CO_2 adsorption of activated carbons at 273 K was studied by Grand Canonical Monte Carlo (GCMC) simulations depicting the adsorption mechanism by micropores and mesopores as shown in Figure 3 [86]. The snapshots of pores of 6.3 and 6.5 Å widths show the formation of a single layer, also known as a monolayer, of carbon dioxide molecules with the molecules lying horizontally parallel to the surface. When pressure is increased over 100,000 Pa, CO_2 starts to penetrate voids in the carbonaceous surface, becoming fully packed at saturation pressures. On the other hand, in the mesopore range, a first layer is completed at low pressure, with pressures higher than 500,000 Pa, a second layer is formed, and voids in the AC surface are filled with CO_2 molecules. When the second layer is filled, the short-range intermolecular forces between the surface and adsorbate are negligible, and pore filling is carried out by capillary condensation.

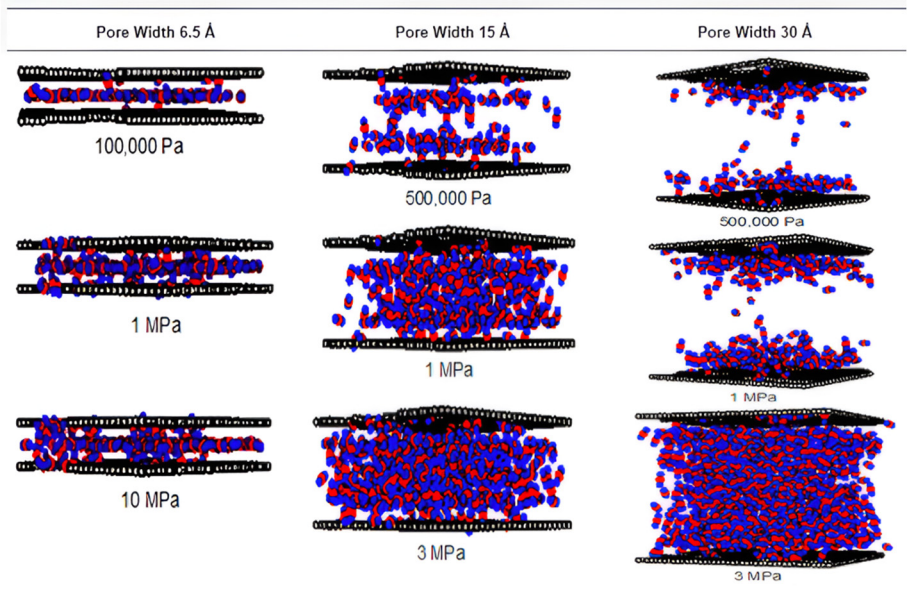

Figure 3. Snapshots of CO_2 adsorbed in finite-length carbon slit pore with defective surface using GCMC simulation at 273 [86]. Black spheres represent AC carbon atoms; red and blue spheres correspond, respectively, to carbon and oxygen atoms in CO_2.

2.2. Influence of Textural Properties

Textural properties, comprising the physical characteristics of the adsorbent that determine its microstructure and morphology, are therefore crucial to defining the adsorption behavior of activated carbons. They are the most influential parameters that define the material capacity to capture and retain carbon dioxide during the biogas upgrading process. They also govern the maximum adsorption capacity, the number of available surface sites for adsorption, as well as the size distribution of pores, which are relevant factors for carbon dioxide adsorption and separation.

Activated carbons◎textural properties are highly dependent on the substrate composition and preparation method, in such a way that they can be tuned to enhance the adsorption properties. Carbon dioxide adsorption capacities of activated carbons can reach values of 5.24 mol CO_2/g with good removal efficiencies from biogas, allowing biogas enrichment from 61 to up to 91% methane purity [91]. Understanding the role that each parameter has on the adsorption behavior of ACs is of great importance for the development of optimized adsorbents with industrial potential applicability.

2.2.1. Specific Surface Area (SSA)

This measures the total surface area of the adsorbent per unit of mass, and it is typically reported in square meters per gram ($m^2\ g^{-1}$). A higher value of SSA means more available accessible area for adsorbate–adsorbent interactions, which translates into more active sites for the adsorption of molecules. Large surface areas are related to enhanced adsorption capacities [92]. Activated carbons can present surface areas of up to 3000 $m^2\ g^{-1}$, which makes them suitable materials for adsorption-based industrial processes.

SSA is commonly measured by the Brunauer–Emmett–Teller (BET) method, which consists in obtaining the nitrogen adsorption isotherm at 77 K of the adsorbent, and the surface area is then calculated from the gas adsorbed volume. The obtained value is known as BET surface area (S_{BET}) [93]. Textural properties of different activated carbons reported in the literature, including S_{BET}, are shown in Table 1.

Table 1. Effect of textural properties on the carbon dioxide uptake capacity of activated carbons as reported in the literature.

Sample (Substrate)	S_{BET} ($m^2\ g^{-1}$)	V_{Tot} ($cm^3\ g^{-1}$)	V_{micro} ($cm^3\ g^{-1}$)	$V_{<0.7\ nm}$ ($cm^3\ g^{-1}$)	CO_2 Uptake (mmol g^{-1}) at 298 K	Reference
AC-1 (anthracite)	1004	0.48	0.23 [a]		3.16	[94]
AC-4 (anthracite)	1394	0.67	0.32 [a]		3.49	[94]
AC-2 (anthracite)	1615	0.80	0.22 [a]		2.77	[94]
CC2-800 (cotton fiber)	1371	0.609		0.3361	4.43	[95]
CC3-800 (cotton fiber)	1343	0.600		0.2568	3.75	[95]
CHPA-2-750-f Chestnut shell)	1792	0.729	0.293	0.297	13.36	[96]
Bamboo-1-1073	1273	0.51	0.31		5.9 [b]	[58]
Bamboo3-973	2332	1.00	0.37		7.0 [b]	[97]
Bamboo-5-973	2980	1.41	0.28		5.3 [b]	[97]
MCC	648	0.299	0.266	0.218 [c]	2.28	[98]
MCC-K1	916	0.432	0.367	0.25 [c]	2.42	[98]
MCC-K2	1057	0.581	0.474	0.271 [c]	2.77	[98]

[a] Volume of pores under 0.1 nm. [b] Measured at 273 K and 1 bar. [c] Pore volume under 0.8 nm.

The influence of the surface area on the adsorption capacity was studied by Cui et al. [99] by comparing the carbon dioxide uptake by nine activated carbons produced from glucosamine hydrochloride with different textural properties. The ACs showing BET surface areas higher than 2000 $m^2\ g^{-1}$ showed superior carbon dioxide adsorption capacities with values ranging from 17.08 to 18.63 mmol g^{-1} at 2 MPa and 298 K. Under the reported

adsorption conditions, a correlation of $R^2 = 0.773$ was found between the BET surface area and CO_2 uptake, signaling a high influence between surface area and adsorption capacity at high adsorption pressures.

Similar results were found by B. Ruiz et al. by analyzing eight activated carbons produced from chestnut shells [96]. S_{BET} values were calculated to be in the range between 1117 and 1792 $m^2\ g^{-1}$. A correlation factor of $R^2 = 0.956$ was found between BET specific surface area and the CO_2 uptake at 3 MPa and 273 K. In the low-pressure range ($P < 0.5$ MPa), the presence of higher micropore volumes was reported to enhance the CO_2 adsorption capacity. Other textural parameters found to influence the CO_2 adsorption behavior were total pore volume, medium micropore volume, and mean micropore size.

By studying a set of three activated carbons produced from anthracite under different activation conditions, Li et al. depicted the influence of BET surface area, pore volume, and narrow micropore volume (>1 nm) on carbon dioxide adsorption for biogas upgrading [94]. Their results indicate that the maximum carbon dioxide adsorption capacity is obtained when surface area and narrow micropore volume are increased to values of 1394 $m^2\ g^{-1}$ and 0.32 $cm^3\ g^{-1}$, respectively. A further increase in surface area while maintaining a narrow micropore volume indicates the creation of wider pores inside the carbonaceous structure. This is because, due to the weak character of the interactions involved in gas adsorption by activated carbons, the adsorbate molecules cannot be retained on the surface.

Wei et al. analyzed the influence of BET surface area on carbon dioxide adsorption for a series of fifteen ACs produced using bamboo as precursor [97]. Their results show that adsorption capacity at 0.1 MPa increased with increasing SSA of up to 2000 $m^2\ g^{-1}$; however, further increases in SSA proved to be detrimental to adsorption capacity, with activated carbons with surface areas between 2000 and 3000 $m^2\ g^{-1}$ showing progressively lower adsorption capacities with higher surface areas. High correlation factors ($R^2 > 0.8$) were found between CO_2 adsorption at low pressure and the volume of micropores in the range of 0.33–0.90 nm in the work.

2.2.2. Pore Size Distribution (PSD) and Pore Volume

PSD describes the range and proportions of pore sizes within the adsorbent, thus providing insights into the accessibility of the porous structure for the adsorbate molecules. This parameter describes not only the average pore size but also the distribution shape, indicating if the material has a narrow distribution, similar pore sizes, or a wide distribution, varying range of pore sizes. Its measurement is highly relevant for the study of adsorption properties, since, as already discussed, different pore sizes are related to mass transfer and molecular sieving effects and thus highly influence the adsorption properties of the adsorbate–adsorbent pair. Pore sizes are categorized into three main categories: micropores (pore diameter less than 2 nm), mesopores (pore diameters from 2 nm to 50 nm), and macropores (pores with diameters larger than 50 nm).

Activated carbons tend to have a developed microporous structure as depicted in Figure 4 for four activated carbons prepared from avocado stones by chemical activation using sulfuric acid [100]. The PSD profiles obtained for the samples show two main peak regions, indicating the predominant presence of pores with sizes under 1 nm and a lower presence of pores from 1.0 to 1.5 nm. The presented figure also highlights the effect of activation conditions upon the development of the porous structure of AC, with the activation temperature varying from 700 to 750 and 800 for C_H_2SO_4_1.5_700, C_H_2SO_4_1.5_750 and C_H_2SO_4_1.5_800, respectively, while C_H_2SO_4_1.5_700 and C_H_2SO_4_1_700 were both prepared under the same activation temperature but with different mass ratio avocado stone: H_2SO_4 for the first sample it was 1.5 and 1.0 for the second

AC. The effect of activation conditions for a given method on the adsorption properties of carbon dioxide by ACs is further discussed in Section 3.

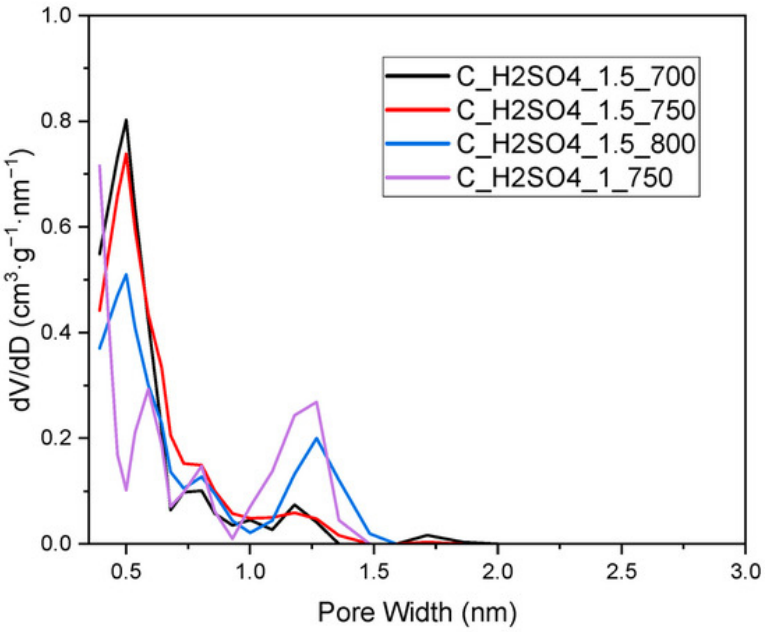

Figure 4. Pore size distribution of activated carbons, prepared from avocado stones and activated by H_2SO_4, determined using the DFT method based on N_2 sorption at 77 K (source: [100]).

By integrating the pore size distribution curve obtained over the entire pore size range for each adsorbent, the total pore volume (V_{TOT}) can be calculated. Total pore volume can also be measured by intrusion of mercury under controlled pressure (MIP) [101], water displacement, and gas pycnometry with helium or nitrogen [102]. Furthermore, the volume of pores with a particular size range, i.e., the volume of micropores (V_{micro}), can be extracted from the N_2 adsorption isotherms and the corresponding PSD profiles. Both V_{Tot} and V_{micro} are measured in $cm^3\ g^{-1}$.

The adsorption of CO_2 by ACs driven by non-specific short-range interactions is carried out by a pore-filling process. When pore sizes are in the micropore range, the adsorption potential of each parallel adsorption plaque overlaps, enhancing the pore filling. Therefore, the adsorption process is highly dependent on the volume of pores in each size range [103]. In particular, the presence of narrow micropores (<0.8 nm) has been reported to be the dominant factor for CO_2 adsorption at low pressure.

Hong et. al [98] found a very close correlation between the volume of the narrow micropores (<0.8 nm) and CO_2 adsorption capacities at different temperatures for a set of six Wheat-Derived Activated Microporous Carbons obtained by chemical activation with different activation agent ratios (see Figure 5). Total pore volume and micropore volume were not well related to CO_2 adsorption capacities, especially when an increase in these properties meant a reduction in narrow micropore volume by a pore enlargement mechanism. In a similar manner, their results show an enhancement of CO_2 adsorption with increasing BET surface areas of up to 1500 $m^2\ g^{-1}$, followed by a decrease in the CO_2 adsorption for higher BET surface areas linked to a smaller volume of pores under 0.8 nm.

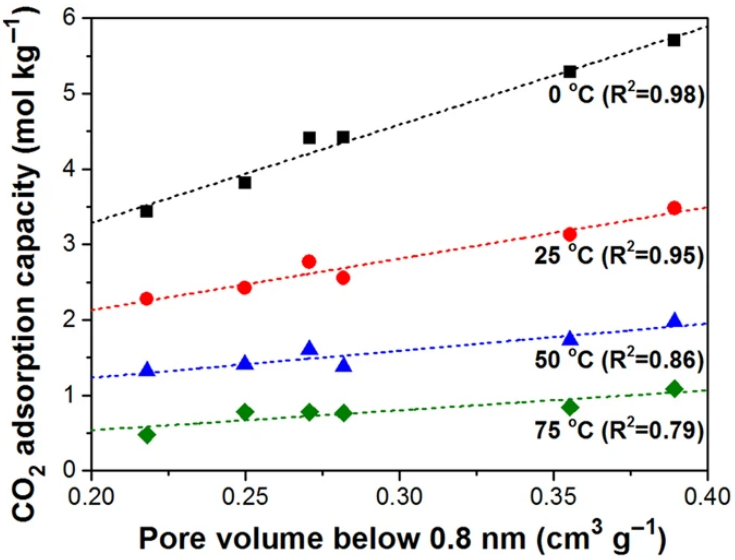

Figure 5. Correlation between CO_2 adsorption capacities at 0.1 MPa and volume of narrow micropores with a pore size of less than 0.8 nm at different temperatures for Wheat-Derived Activated Microporous Carbons produced by chemical activation with varying mass ratios of KOH (source: [98]).

Taking into consideration pore sizes in the range of 0.3–1.4 nm, Serafin et al. characterized the effect of narrow micropore size distribution of activated carbons derived from different biomass on CO_2 adsorption at 273 and 298 K and 0.1 MPa [104]. The volume of micropores in the range of 0.30–0.86 nm was crucial for CO_2 adsorption at 273 K; however, when the adsorption temperature increased to 298 K, the best linear relationship was found for pore volumes in the range 0.30–0.33 nm, close to the kinetic diameter of CO_2.

At higher pressures, adsorption follows capillary condensation and liquefaction of gas molecules inside wider pores, thus resulting in broader pores contributing to an enhancement of the adsorption capacity at high adsorption pressures. CO_2 adsorption by AC at pressures over 0.1 MPa has been shown to correlate with surface area, total pore volume, and volume of pores of a wider range. Ruiz et al. found a correlation value of 0.9563 between medium micropore volume (pore volume with pores of 0.7–2 nm) and CO_2 adsorption capacity at 298 K and 3 MPa for a set of eight AC [96]. On the same work, R^2 values of 0.9938 and 0.9668 were found for the linear relation between S_{BET} and V_{TOT} with CO_2 adsorption capacity, respectively.

Peredo et al. [105] also reported good correlation values between carbon dioxide maximum adsorption capacity and BET surface area ($r^2 = 0.959$) for a set of five commercial activated carbons; micropore volume also showed to have an important influence on the adsorption capacity at high pressure ($r^2 = 0.883$).

By analyzing 1300 data points from the literature via deep neural networks, Mehrmohammadi and Ghaemi investigated the impact of textural properties, particularly micropores, on CO_2 adsorption capacity on porous carbon materials [106]. Their results show a high influence of micropore volume in the range of carbon dioxide adsorption at low pressure (0.1–0.5 MPa) (see Figure 6). On the other hand, at pressures of 1.5 and 2.0 MPa, adsorption on mesopores is depicted by higher CO_2 uptakes within the mesopore volume range of 4–8 cm^3 g^{-1}, attributed to the saturation of micropores at higher pressures, necessitating the contribution of mesopores to achieve higher CO_2 uptake.

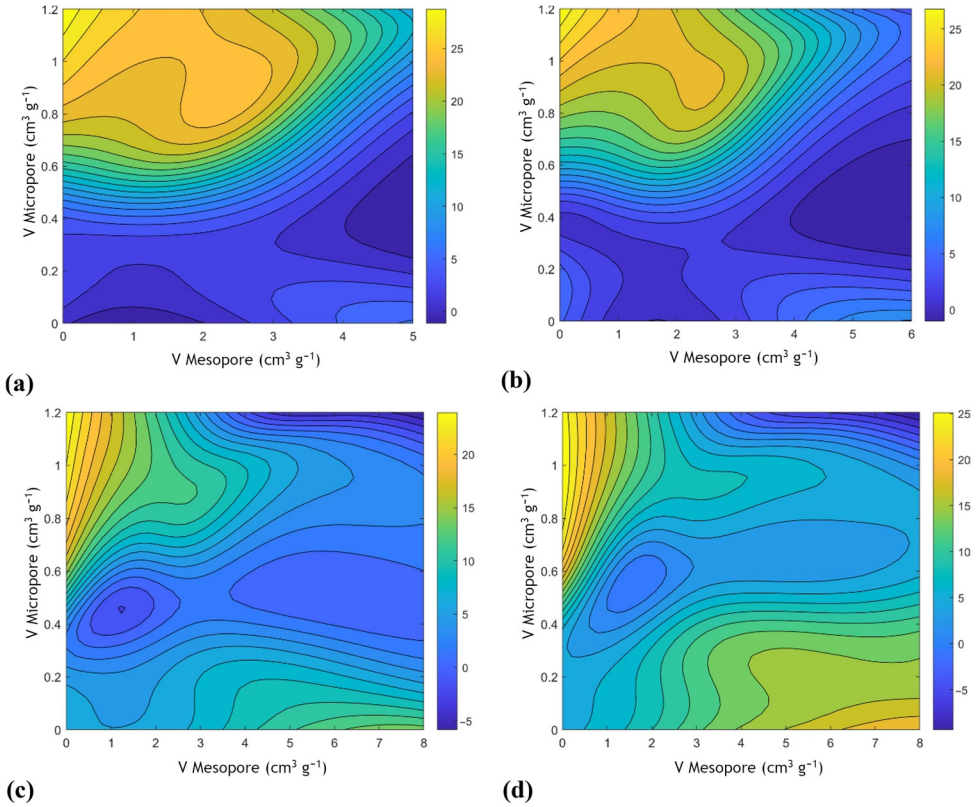

Figure 6. CO_2 adsorption contours based on mesopore and micropore volume for MLP deep network with LM training algorithm at pressures (**a**) 0.1 MPa, (**b**) 0.5 MPa, (**c**) 1.5 MPa, (**d**) 2 MPa (source: [106]).

In addition, some authors have signaled the importance of also measuring the ultramicropore volume (pore diameter lower than 0.7 nm) as it has been reported to enhance the CO_2 adsorption and selective separation [107–109]. Common methods to measure the PSD include Barret–Joyner–Halenda (BJH) method applied to BET adsorption isotherms, Mercury Intrusion Porosimetry (MIP) [110], Nuclear Magnetic Resonance (NMR) [111], Small Angle X-ray Scattering (SAXS) [112], and Molecular Simulations, such as Density Functional Theory (DFT) [113] and Grand Canonical Monte Carlo (GCMC) [114].

2.3. Influence of Chemical Composition and Surface Chemistry

Gas adsorption requires the adhesion or binding of the adsorbate molecules on the surface of the adsorbent. Depending on the surface chemistry, the interaction forces will be stronger, such as chemical bonding (chemisorption) or weaker, involving van der Waals forces (physisorption) [101]. When the adsorbate is constituted by more than one type of molecule, the ability to selectively adsorb one probe over another can be influenced by the strength of the attraction/repulsion forces between the surface and each of them. Furthermore, the reversibility of the adsorption process during the adsorbent regeneration is also affected by the surface chemistry.

To produce a highly purified methane stream from biogas by adsortpion-based separation methods such as Pressure Swing Adsorption (PSA) and Vacuum Swing Adsorption (VSA), the adsorbent material has to have a large working capacity, as well as a high CH_4/CO_2 selectivity factor ($S_{CH4/CO2}$), defined by Equation (1):

$$S_{CH4/CO2} = \frac{X_{CO2} \cdot Y_{CH4}}{X_{CH4} \cdot Y_{CO2}} \quad (1)$$

where X refers to the molar fraction of the compound in the adsorbed state, and Y is the molar fraction of this compound in the gas phase. For biogas upgrading, methane, a non-

polar molecule, can only be absorbed by physisorption, while the quadrupole moment of carbon dioxide results in its ability to interact through electrostatic interactions [102]. Adsorbent materials with surface electron donor groups can enhance the CO_2 adsorption through stronger hydrogen bonding and acid–base interaction, which translates into a higher CH_4/CO_2selectivity factor [115]. Some primary techniques used for chemical surface characterization of adsorbents include X-ray Photoelectron Spectroscopy (XPS) [116], Energy Dispersive X-ray Spectroscopy (EDX) [117], Fourier Transform Infrared Spectroscopy (FTIR) [118], and Thermal Programmed Desorption Mass Spectrometry (TPD-MS) [119].

To enhance the adsorption selectivity of AC, several authors have studied the introduction of heteroatoms such as nitrogen, sulfur, and phosphorus through post-synthesis treatment of ACs. This subject is discussed below in Section 4.

2.4. Section Summary

Activated carbons have textural and chemical properties that make them attractive candidates for biogas upgrading. ACs adsorb carbon dioxide molecules by short-range weak interactions that arise from temporary fluctuations in the electronic distribution around molecules, producing instantaneous dipoles. At low adsorption pressures, the presence of ultramicropores (pores under 0.7 nm) as well as surface basic functionalities has a positive impact on the carbon dioxide adsorption capacity and CH_4/CO_2 selectivity. On the other hand, at pressures over 1 MPa, the total pore and BET surface area also play an important role in the adsorption behavior. Identifying the impact of these properties is crucial for the optimization of ACs.

3. Factors Influencing the Properties of Activated Carbons Relevant for Biogas Upgrading

Both the adsorption capacity and adsorption selectivity of the activated carbons are dependent on the substrate and the activation process (activating agent and activation conditions). Specific activation methods, the activation conditions, and the activator agent define the development of porosity inside the adsorbent structure. The present section revises the effect of each of these factors on the adsorption behavior of ACs, as discussed in the literature.

3.1. Substrate

For biogas upgrading, ACs have been shown to selectively adsorb CO_2 from CH_4/CO_2 mixtures, as well as having important advantages that make them suitable materials for Biogas Upgrading [120]. Most common precursor sources on a commercial scale of ACs include wood, anthracite, bitumen charcoal, lignite, peat shell, and coconut; all these materials show a carbon content higher than 40%, low inorganic content, and good percentage yields, as shown in Figure 7 [121].

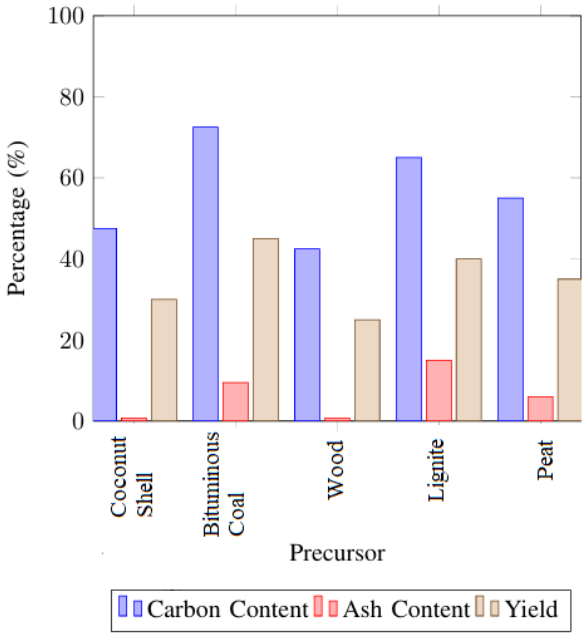

Figure 7. Comparison of key properties of activated carbon precursors [121].

The selection of the substrate depends on the desired final characteristics of the ACs, as well as economic factors, and more recently, sustainability considerations. In this context, environmental concerns and the search for cost-effective alternatives have motivated the development of new alternative precursors that can reduce the environmental impact of AC while achieving competitive CO_2 adsorption performances. Biomass-derived activated carbons (BDAC) have had a growing interest as a cheap alternative with additional environmental advantages and high yield rates. Furthermore, BDAC obtained from organic residues allows the recovery of organic wastes from different sources, simultaneously promoting sustainability in biogas systems while mitigating waste management impacts, further enhancing the circular economy [122,123]. Table 2 presents different biomass-based ACs and their reported CO_2 adsorption capacity and CH_4/CO_2 adsorption selectivity.

Table 2. Biomass-based activated carbons reported textural properties and CO_2 adsorption capacities.

Precursor	S_{BET} ($m^2\ g^{-1}$)	V_{Tot} ($cm^3\ g^{-1}$)	V_{micro} ($cm^3\ g^{-1}$)	Yield (%)	CO_2 Max. Uptake (mol kg^{-1}) at 298 K	$S_{CH4/CO2}$	References
Bamboo	1846	0.78	0.36	21.7	7.0	8.5	[97]
Coconut shell	1105	0.35	0.34		7.59	6.5	[120]
Olive stones	1178	0.49	0.45	-	10.873	-	[124]
Avocado stones	538	0.217	0.175	21	4.9142 (293 K)	-	[100]
Chestnut shell	1792	0.729	0.295	34.14	13.36	-	[96]
Defatted grape seeds	1604	0.672	0.250	-	11.48	-	[125]
Date seeds	798.38	-	0.28	7.25	2.9	-	[126]
Babassu coconut	809	0.39	0.32	14.6	10.49	4.2	[127]
Almond shell	326	0.24	0.23	24	2.18	-	[122]
Cherry stone	1045	0.48	0.40	-	10.88	3.61	[123]
Peanut shell	956	0.77	-	-	4.03	-	[128]
Sunflower seed	1790	0.43	-	-	4.61	-	[128]

The selection of the precursor material significantly influences the properties and performance of the final product, this was evidenced by Serafin et al. by comparing ACs produced from different biomass precursors (Pomegranate peels, tinder fungus:

Piptoporus betulinus, *Trametes versicolor* (L.) Lloyd, mistletoe branches and leaves, carrot peels, kiwi fruit peels, fern leaves, sugar beet pulp) using the same activation method and activation conditions (chemical activation with KOH by impregnation at a mass ratio of 1:1 KOH/dry substrate followed by carbonization at 973 K) [104]. The ACs showed BET surface areas that ranged from 585 $m^2\ g^{-1}$ to up to 1699 $m^2\ g^{-1}$; total pore volume and micropore volume were also highly impacted, ranging from 0.28 cm^3/g and 0.20 cm^3/g to 0.80 $cm^3\ g^{-1}$ and 0.54 $cm^3\ g^{-1}$, respectively. Table 3 shows the obtained textural properties and CO_2 uptake at 1 bar and 298 K of the three ACs that showed better CO_2 adsorption capacities. The work reports the cumulative micropore volume in the range 0.30–0.33 nm to show the best linear relationship between textural parameters and CO_2 adsorption capacity. In the work, total pore volume and BET surface area did not correlate with the adsorption capacity of the studied samples.

Table 3. Textural properties and CO_2 uptake at 1 bar and 298 K for activated carbons produced from biomass as reported by [104].

Substrate	S_{BET} ($m^2\ g^{-1}$)	V_{tot} ($cm^3\ g^{-1}$)	V_{mic} (N_2) ($cm^3\ g^{-1}$)	CO_2 Uptake
PP	585	0.28	0.2	4.11
CP	1379	0.58	0.51	4.18
FL	1593	0.74	0.54	4.12

Similarly, using the same activation method and conditions, Vilella et al. showed the impact of the substrate on defining the adsorption properties of the resulting activated carbon. The authors obtained two AC by CO_2 physical activation at 1173 K using coconut shells and babassu coconut as carbonaceous precursors. The ACs showed significant differences in the textural properties: surface area of 1452 $m^2\ g^{-1}$ and 809 $m^2\ g^{-1}$, and total pore volume of 0.65 $cm^3\ g^{-1}$ and 0.39 $cm^3\ g^{-1}$ for coconut shell and babassu coconut, respectively [127].

3.2. Influence of the Activation Method

Two main methods are distinguished for AC production (see Figure 8): (a) chemical activation, the precursor is impregnated with an activated agent and then carbonized at low temperatures, activated agents include KOH, H_3PO_4 and $ZnCl_2$; (b) physical activation, the precursor is carbonized at temperatures ranging from 773 to 1073 K to remove non-carbonaceous atoms, followed by activation with an oxidizing agent, such as steam or carbon dioxide, at a high temperature (973 to 1273 K) [129].

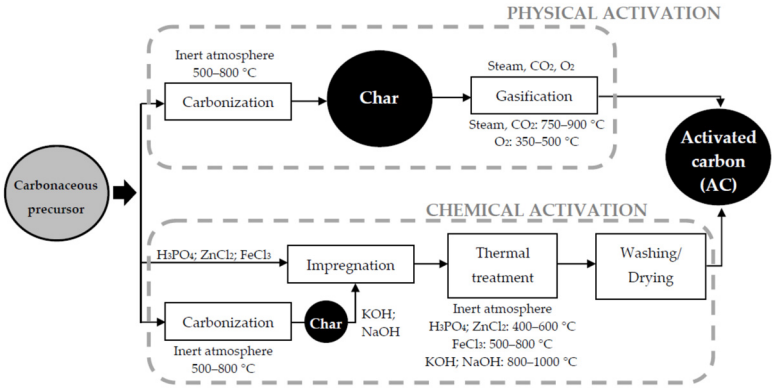

Figure 8. Synthesis of activated carbons (Source: [130]).

Chemical activation usually requires lower activation temperatures and is related to higher yields. Another advantage of chemical activation is that it allows a very precise

control and tailoring of the resulting textural properties by controlling the activation parameters. However, the main drawback of this technique is the corrosiveness and environmental risk of the chemical agents involved and the byproducts obtained during the washing of the adsorbent to remove any remains of the activation agent [131].

Activation parameters can have a major impact on the definition of the textural properties of the adsorbent obtained with a given activation method and activating agent. Factors such as the activation temperature and the activating agent/biomass weight ratio need to be carefully evaluated in order to optimize the adsorption behavior of AC. Table 4 highlights the effect that these parameters can have on CO_2 uptake for Biogas Upgrading.

Table 4. Effect of activation method and activation conditions on CO_2 uptake by activated carbons as presented in the literature. Some of the reported values were derived from graphical data; slight inaccuracies compared with actual values may exist.

Sample (Precursor)	Activation Method/Conditions	CO_2 Uptake (mol kg^{-1})	Ref.
Olive stones	1. Physical: Carbonization at 873 K and H_2O activation at 1023 K	(T = 303 K) 7.968	[124]
	2. Physical: Carbonization at 873 K and H_2O activation at 1023 K	5.878	
	3. Chemical: H_3PO_4 impregnation at a weight ratio of 1:3 at 383 K.	10.873	
Post-consumer plastic waste	Chemical: Pyrolysis at 450 or 500 °C and activation at 1:1 mass ratio with:	(T = 298 K)	[57]
	• KOH 450 and 500 °C,	41.3/84.8 mg g^{-1}	
	• NaOH 450 and 500 °C,	29.2/29.1 mg g^{-1}	
	• K_2CO_3 450 and 500 °C,	67.6/82.1 mg g^{-1}	
	• Na_2CO_3 450 and 500 °C,	64.1/58.3 mg g^{-1}	
	• $FeCl_3$ 450 and 500 °C,	33.7/43.5 mg g^{-1}	
	• $ZnCl_2$ 450 and 500 °C.	34.6/29.8 mg g^{-1}	
Olive stones	Chemical: Carbonization at 500 °C and impregnation at a mass ratio of 1:1 with:	(T = 303 K)	[132]
	saturated KOH,	4.33	
	85% H_3PO_4,	4.00	
	KOH solution from banana peels extract	3.58	
Pomegranate peel	Chemical: One-step activation with K_2CO_3 activating agent in proportions of 0.5:1 and 1:1 at varying temperatures:	(T = 298 K)	[133]
	• 0.5:1 at 850 °C,	11.8	
	• 0.5:1 at 900 °C,	13.0	
	• 0.5:1 at 950 °C,	15.1	
	• 1:1 at 850 °C,	12.4	
	• 1:1 at 900 °C,	13.7	
	• 1:1 at 950 °C.	16.3	
Chestnuts shells	Chemical: Carbonization at 750 °C followed by KOH impregnation in weight	% mass fraction	[96]

	ratios of 1:1. and 2:1 and different temperatures:		
	• 1:1 at 750 °C,	35%	
	• 1:1 at 800 °C,	42%	
	• 1:1 at 900 °C,	51%	
	• 2:1 at 750 °C.	58%	
Coconut shell	Physical: Carbonization at 850 °C followed by CO_2 activation at 750 °C until different burn-offs:		[134]
	• 25%	4.8/2.3 mmol cm^{-3}	
	• 35%	5.0/2.3 mmol cm^{-3}	
	• 52%	4.9/1.9 mmol cm^{-3}	
	• 79%	4.8/1.5 mmol cm^{-3}	
	• 94%	4.9/1.3 mmol cm^{-3}	
Almond Shell	Physical: Activation with air at two temperatures and different reaction times:	(298 K)	[135]
	• 400 °C and 28 min,	1.14	
	• 400 °C and 40 min,	1.29	
	• 400 °C and 42 min,	1.37	
	• 450 °C and 26 min,	1.51	
	• 450 °C and 32 min,	1.57	
	• 450 °C and 36 min,	1.53	
Cellulose	1. Hydrothermal activation with amines at 240 °C:	(273 K)	[136]
	• diethylenetriamine (DETA),	4.38	
	• 1,2-bis(3-aminopropylamino)ethane (BAPE),	5.33	
	• melamine (MELA).	7.34	
	2. Hydrothermal activation with amines, KOH activation and carbonization at 800 °C:		
	• diethylenetriamine (DETA),	1.76	
	• 1,2-bis(3-aminopropylamino)ethane (BAPE),	2.19	
	• melamine (MELA).	4.16	
Cherry stones	Physical: single step activation with:	(303 K)	[137]
	• CO_2	5.14	
	• H_2O vapor	4.48	
Sugarcane	Physical: carbonization at 750 °C and activation at carbonized at 850 °C with:	(298 K)	[138]
	• Air	1.6	

• CO_2	2.6
Chemical: direct pyrolysis and activation of the precursor impregnated with:	
• H_3PO_4	2.7
• NaOH	4.3

The effect of the activation method and activation agent (chemical: H_3PO_4, $ZnCl_2$ and physical: CO_2) on the textural properties of the activated carbon was tested by Arami et al., their results show that samples obtained by chemical activation with phosphoric acid followed by activation with carbon dioxide, showed overall higher surface areas and micropore volumes that those for zinc chloride followed by carbon dioxide [139]. Furthermore, physically activated carbons had a comparable surface area to that of the carbons obtained using $ZnCl_2$ chemical activation. On the other hand, physical activation resulted in a higher degree of heterogeneity of the pore size distribution.

Peredo et al. also analyzed the effect of the activation method on CH_4 and CO_2 adsorption for BDAC obtained from olive stones by physical activation (CO_2 and H_2O) and chemical activation (H_3PO_4) [124]. Their results show that chemical activation resulted in more developed textural properties (surface area, total pore volume, and micropore volume), which allowed higher intake of carbon dioxide (max. adsorption capacity: 10.873 mol g^{-1}. The main parameter for methane adsorption was found to be the presence of mesopores, which facilitated the diffusion of the gas molecules. All the samples showed higher adsorption capacities of carbon dioxide than those of methane. Furthermore, their findings demonstrated that even if the two physically activated ACs had similar textural properties, their gas uptake differ (7.968 mol g^{-1} for H_2O activation and 5.878 mol g^{-1} for CO_2 activation), explained by the effect of chemical surface groups that also showed to influence the adsorption behavior of the adsorbents, i.e., activation with H_2O resulted in highest content of oxygen surface groups which enhanced the CO_2 adsorption, proving than not only textural properties are relevant for gas adsorption and separation processes, chemical properties of the adsorbent surface are also a relevant parameter that can be optimized to enhance the wanted behavior of the adsorbent.

Krupšová et al. also explored the effect of surface groups on CO_2 adsorption properties. They prepared cellulose-based activated carbons modified with amines: diethylenetriamine (DETA), 1,2-bis(3-aminopropylamino)ethane (BAPE), and melamine (MELA), by (a) hydrothermal and (b) hydrothermal activation followed by chemical activation with KOH and pyrolysis [137]. The samples obtained by the thermal activation method showed overall better textural properties than their counterparts obtained by hydrothermal activation alone, explained by the KOH chemical activation step, which promotes the formation of micro- and mesopores. Furthermore, for the same activation protocol, more enhanced degrees of porosity and BET surface areas were observed on melamine-containing material, followed by samples doped with 1,2-bis(3-aminopropylamino)ethane and finally diethylenetriamine (as shown in Figure 9a). However, carbon dioxide adsorption as measured by the volumetric method at 0 °C showed higher CO_2 adsorption capacities for the samples activated by hydrothermal treatment. The adsorption capacity was found to increase with the increasing number of amine groups (nitrogen atoms) in the formula of amine used as an in situ N-modifying agent, indicating that the CO_2 uptake is dependent on the basicity of the materials in the measured pressure range and temperature.

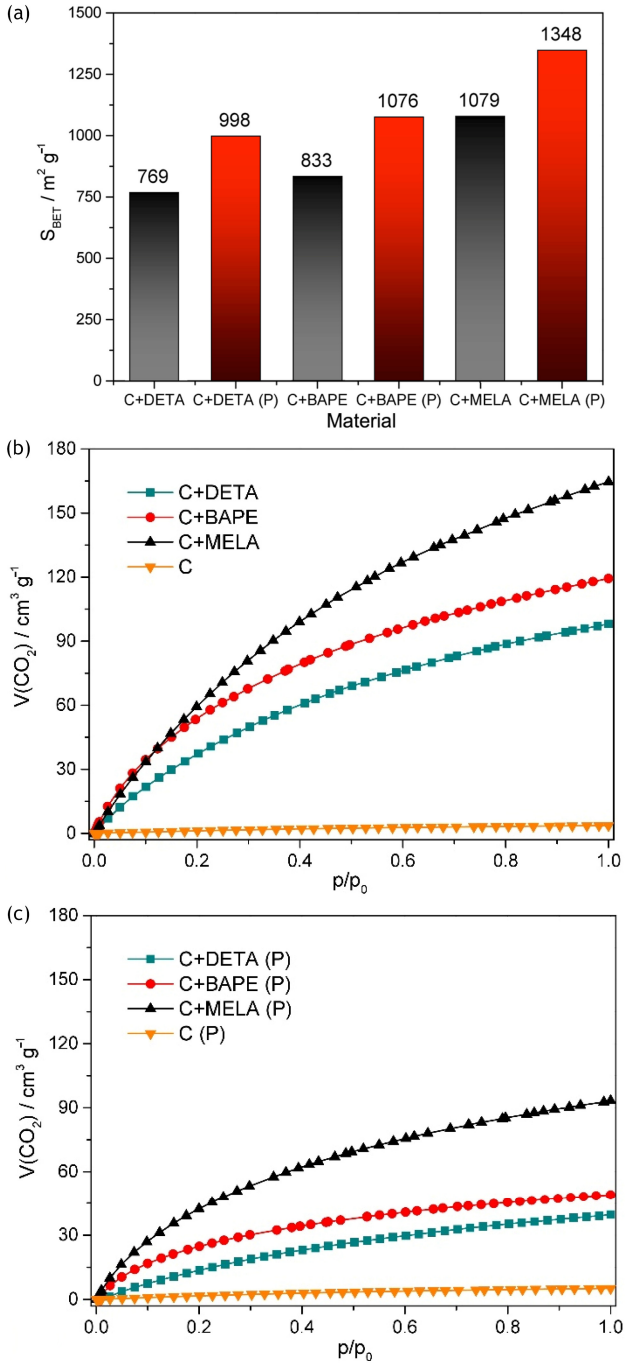

Figure 9. (**a**) Comparison of S_{BET} surface areas for hydrothermal (black columns) and thermal (red columns) samples and CO_2 adsorption/desorption isotherms of (**b**) hydrothermal and (**c**) thermal materials measured at 0 °C and up to 1 bar (source: [137]).

Solís et al. explored the effect of diverse chemical activation agents, K_2CO_3, KOH, Na_2CO_3, NaOH, $ZnCl_2$, and $FeCl_3$, on the CH_4, CO_2, and CH_4/CO_2 mixtures adsorption by activated carbons prepared from post-consumer plastic from the rejection fraction of a municipal solid waste treatment plant [57]. The use of K_2CO_3 displayed better carbon dioxide uptakes attributed to higher ultramicropore volume and oxygenated surface functional groups (see Figure 10). The carried-out dynamic CH_4/CO_2 50/50 (*v*/*v*) adsorption tests depicted close behavior to commercial materials such as zeolites, and a methane yield of up to 95% was achieved. The work opens a new research line for valorizing non-recyclable plastic waste to produce microporous adsorbents for biogas upgrading.

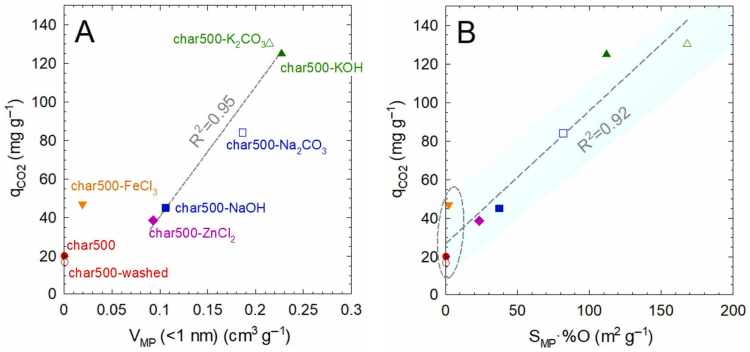

Figure 10. Correlation of the CO_2 adsorption uptake (273 K and 100 kPa) vs. ultramicropore volume HK method (**A**), and correlation of the CO_2 adsorption uptake (273 K and 100 kPa) and the percentage of oxygenated micropores (**B**) for the plastic-based activated carbon prepared from the pyrolyzed char at 500 °C (source: [57]).

The effect of the activation temperature on the resulting activated carbons' textural properties was highlighted by Serafin et al. In the work, activated carbons were synthesized from cashew nut shells by chemical activation with KOH at different temperatures (1073, 1123, and 1173 K) [140]. Their findings showed that upon increasing activation temperature from 1073 to 1123, the resulting activated carbon had more developed porosity (total pore volume 0.847 vs. 0.448 $cm^3\ g^{-1}$) and surface area (1972 vs. 1051 $m^2\ g^{-1}$), however, further activation temperature increase to 1173 resulted in loss of surface area and porosity attributed to some pores collapsing due to excessive temperature. The authors estimated the CH_4/CO_2 selectivity factor for the sample with better textural properties (activation at 1123) of up to 8.4, depicting a pronounced preference for CO_2 adsorption over CH_4.

Chen et al. [58] studied the effect of the activated agent/biomass impregnation ratio for a set of bamboo charcoal-based activated carbons. In the study, they prepared five ACs by chemical activation with KOH using KOH/biomass mass ratios of 0.5:1, 1:1, 2:1, 3:1, and 4:1 at 423.2 K. Textural properties (surface area and total pore volume) increased with higher mass ratios from 0.5:1 to 3:1. The 4:1 ACs showed a decreased in the textural properties. The five AC were almost completely microporous with pores under 2 nm. However, the two ACs produced with the lowest impregnation ratios had more pores under 0.55 nm, indicating that higher impregnation ratios result in the erosion of pores, resulting in wider pores. The study also analyzes the performance of the AC/water hybrid sorbents for Biogas Upgrading, composed of liquid and porous materials, by mixing the obtained AC with H_2O at mass ratios of 1.0, 3.0, and 7.0 wt%, respectively. The best adsorption and separation performance were depicted for the AC with an impregnation ratio of 2:1 and 7 wt%, showing a predicted selectivity of 16, explained by the pore size distribution.

Siemak and Michalkiewicz analyzed the effect of the precursor mass: activating agent ratio and the activation temperature by producing four Avocado stones derived AC using mass ratios of 1 and 1.5 by chemical activation with H_2SO_4 at 700, 750, and 800 °C [100]. The highest values for specific surface area, pore volume, and micropores were obtained for the 750 °C carbonization combined with activation at a mass ratio of 1.5. This sample also showed the highest CO_2 uptake at 0.1 MPa (3.78 mmol g^{-1}), explained by the developed porosity and higher surface area. The activation at 700 °C was found to be insufficient for the development of porosity, while activation at 800 °C resulted in the degradation of the porous structure. On the other hand, reducing the activating agent amount resulted in lower porosity.

Saadi et al. prepared a set of pomegranate peel waste-based ACs by one-step K_2CO_3 chemical activation in proportions of 0.5:1 and 1:1 and activation temperatures of 1123 K, 1173 K, and 1223 K [134]. The resulting adsorbents showed significant textural differences: higher activation temperatures resulted in higher surface areas and total pore volume for both

activation ratios, which translated into higher CO_2 uptakes at pressures higher than 1 MPa. Upon correlation of the adsorption isotherms with the textural parameters of the adsorbents (Figure 11), authors were able to conclude that at low pressures (P < 0.1 MPa) the adsorption mechanism is ultramicropore filling; thus, the ACs with higher narrow micropore volume (under 0.7 nm) showed better uptake at low pressures. On the other hand, at pressures over 0.7 MPa BET surface area, total pore volume, micropore volume, mesopore volume showed a direct relationship with CO_2 capacity, among these properties, mesopore volume and surface area showed higher correlation factors (0.98 and 0.96, respectively) indicating that at high pressure both large and small pores are relevant for gas diffusion and adsorption. Similar findings were depicted for methane adsorption. Nevertheless, all the samples showed a significantly higher CO_2 pure gas adsorption capacity than that for methane.

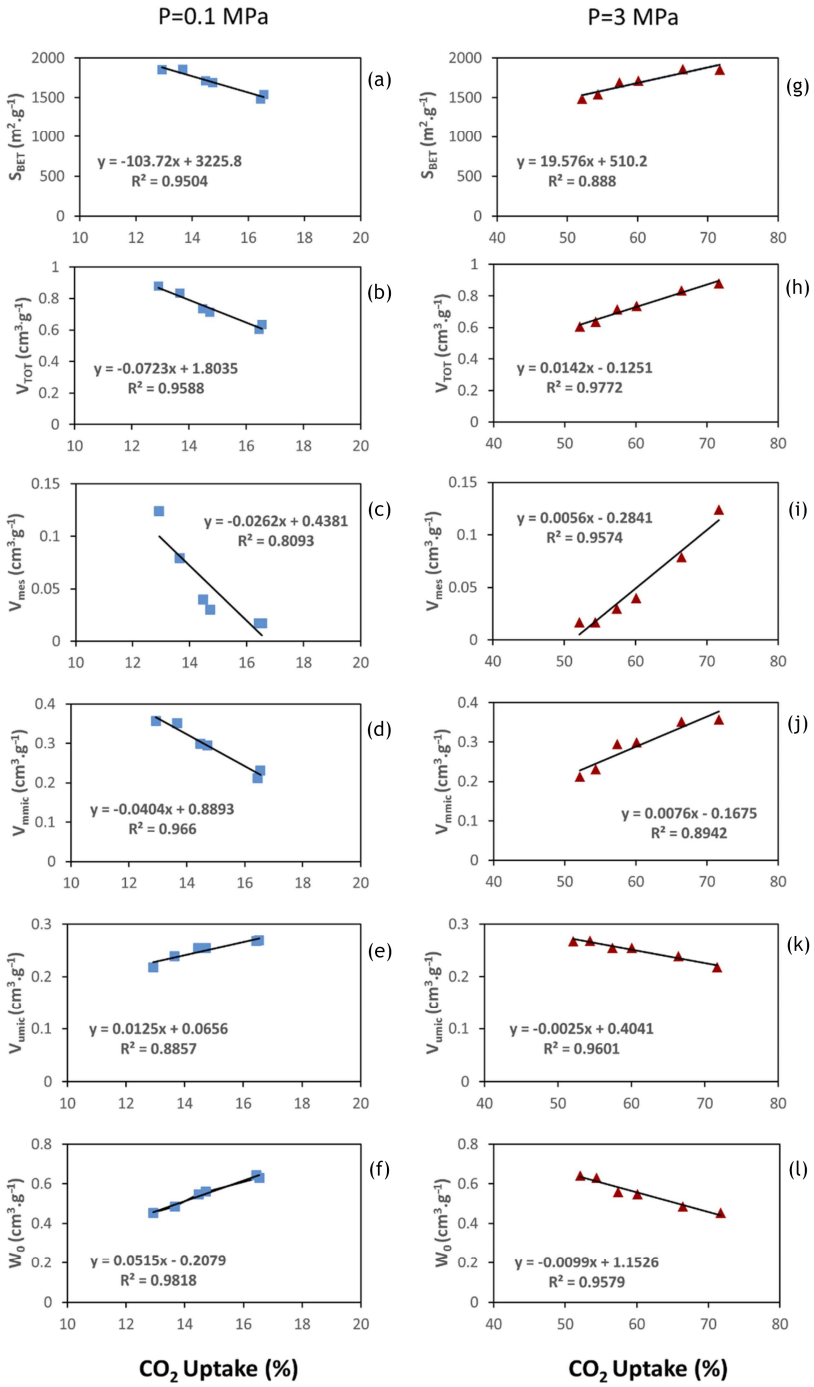

Figure 11. Relationships between textural parameters of the pomegranate peels-based activated carbons and CO_2 uptake at 0.1 MPa (**a**–**f**) and 3 MPa (**g**–**l**). Samples were prepared by a one-step

chemical activation with K_2CO_3 in proportions of 0.5:1 and 1:1 and activation temperatures of 1123 K, 1173 K, and 1223 K (source: [134]).

Ruiz et al. give a comprehensive analysis of how textural properties of ACs can be tuned by choosing the right activation parameters (i.e., activating agent/precursor weight ratio, activation temperature and inert flow gas on the activation process) to meet the requirements for a specific application such as CH_4/CO_2 separation [96]. In order to do so, they obtained sustainable porous carbons from lignocellulosic wastes from the chestnut shell by means of KOH chemical activation. Their results show that increasing the activation temperature from 973 K to 1073 K results in pore widening, in agreement with the previously mentioned works. The ACs obtained at 973 were composed mainly of ultramicropores, while higher activation temperatures resulted in an increase in micropores and mesopores. Similarly, a higher activation agent/precursor weight ratio resulted in wider pores. On the other hand, the inert gas flow rate did not have a particular impact on the textural properties. The carbon dioxide adsorption capacity at 3 MPa was also found to be influenced by the BET surface area, total pore volume, and micropore volume.

Prauchner et al. extended the previous studies from the literature by exploring the effect of the activation conditions during chemical activation with dehydrating agents (H_3PO_4 or $ZnCl_2$) and physical activation with CO_2 systematically [135]. A set of thirty ACs was prepared to this end, and for each activation agent, the effects of temperature, chemical loading, and burn-off were studied. Their findings show that higher burn-offs (physical activation), as well as chemical loadings (chemical activation), resulted in higher total pore volumes due to the creation of mesopores and macropores; however, ultramicropore volume remains almost unchanged. Overall, their results show that physical activation at 1123 K resulted in higher CO_2 gravimetric uptakes, mainly attributed to higher ultramicropore volumes in comparison with chemically activated ACs. Physical activation also resulted in better volumetric uptakes, meaning higher adsorption density. Their systematic scanning of the resulting textural properties correlated with the activating procedures gives light into the mechanisms involved in the development of pores and CO_2 adsorption.

3.3. Section Summary

The adsorption behavior of activated carbons (ACs) in biogas upgrading depends on multiple factors that significantly determine the textural and chemical properties of the adsorbent, such as the substrate, activation method, and activation conditions. Biomass-derived ACs (BDACs) have emerged as sustainable alternatives to conventional precursors, offering environmental and cost advantages. Chemical activation generally results in higher surface areas and micropore volumes than physical activation. Nevertheless, activation conditions such as temperature, activation time, and activating agent ratio also strongly influence the adsorbent performance. Experimental studies reviewed in this section show that minor changes in these parameters can lead to significant variations in the textural and chemical properties of the resulting AC that can translate into an important enhancement of the CO_2 uptake (e.g., from 2.2 to 5.7 mol kg^{-1}).

4. Post-Synthesis Methods for Improving Activated Carbon CO_2 Adsorption and Separation for Biogas Upgrading

Activated carbons can be subjected to post-synthesis treatments to modify and enhance their adsorption capacity and selectivity. In particular, due to the Lewis Acid behavior of carbon dioxide, introducing basic surface functionalities on the adsorbent has been reported to favor CO_2 adsorption [141]. Different modification methods have been proposed in the literature (see Table 5), including N, S, and Ni doping.

Table 5. Post-treatments for activated carbons derived from various precursors.

Precursor	Post-Treatment	Reference
Palm shell	Immersion for 3 days in chitosan solutions with initial concentrations of 0.1–2.0 g/L	[142]
Waste tea	Immersion in 5 mL of 3% *w*/*v* of EDA in methanol	[143]
Petroleum pitch	Treatment with H_2S at elevated temperatures (600 °C and 800 °C) Pre-oxidation treatment with plasma followed by H_2S treatment at elevated temperatures (600 °C and 800 °C)	[144]
Commercial AC	Air oxidation at 400 °C for 2 h, Pre-oxidation treatment followed by immersion in NH_4OH for 36 h	[145]
Polyacrylonitrile	Mixing with sulfur in a 1:1 weight ratio for 1 h at 553 K	[146]
Commercial AC	I. Activation in HNO_3, sequentially activated in tin chloride ($SnCl_2$) and palladium chloride ($PdCl_2$) and nickel dipping into a nickel bath II. Activation in HNO_3, sequentially activated in tin chloride ($SnCl_2$) and palladium chloride ($PdCl_2$) and nickel dipping into a nickel bath, followed by oxidation at 573 K in an air stream	[147]
Commercial AC	I. Mixing with HNO_3 M II. Mixing with HNO_3 M followed by treatment with urea solution 1 M III. Mixing with HNO_3 M followed by treatment with urea solution 1 M and thermal treatment	[92]
Commercial AC	Mixing with a saturated solution of ammonium sulfate salt at different AC/ammonium sulfate mass ratios ($w_{(NH4)2SO4}$ = 4.76, 6.98 and 9.1%)	[59]

Rattanaphan et al. produced an activated carbon from waste tea from a local tea shop by chemical activation with KOH [143]. The sorbent was then modified by immersion in ethylene diamine (EDA). The resulting modified carbon showed a higher concentration of basic nitrogen functionalities, which resulted in a loss of surface area due to pore filling by entrapment of EDA molecules. Nevertheless, their results show an increase in CO_2 pure gas adsorption capacity, as well as a higher CO_2 adsorption capacity from a real biogas stream. To explain the behavior, the team carried out Density Functional Theory (DFT) analysis, from which stronger adsorption energies between carbon dioxide and the modified surface structures than those obtained for the unmodified carbon were calculated .

In this context, the application of molecular simulations to predict or explain specific interactions between surface groups and the adsorbate molecules has become a powerful tool to support and facilitate gas adsorption and separation experimental analysis. Using a combination of DFT and Grand Canonical Monte Carlo (GCMC) simulations, Lu et al. investigated the effect of edge-functionalization on nanoporous carbons◎CH_4/CO_2 competitive adsorption [148]. Their results show that adsorption selectivity towards carbon dioxide is enhanced by adding surface groups in the order of NH_2 > COOH > OH. The increased selectivity is attributed to electrostatic interactions, stronger adsorption energies, and high electronegativity/electropositivity. The improvement in selectivity was

shown to be unaffected by temperature increases in the gas phase; however, it does rapidly decrease when the working pressure is increased.

Phalakornkule et al. studied the effect of chitosan surface modification of a palm-shell-based AC. To this end, native carbon was impregnated with chitosan at a 0.76% weight. Their results show an important improvement in biogas upgrading dynamic tests in comparison with the results obtained for the native carbon. Mainly, the MAC was able to maintain CH_4 breakthrough purity of 100% during the consecutive adsorption cycles, while the native ACs showed a sooner breakthrough of carbon dioxide, which lowered the purity of the methane stream after the second cycle [143].

Reljic et al. analyzed the performance of a petroleum pitch-based activated carbon produced by chemical activation with KOH before and after a post-treatment with H_2S [144]. In the work, two modification methods were proposed: (a) direct treatment with H_2S at elevated temperatures (600 °C and 800 °C), and (b) pre-oxidation treatment with plasma followed by H_2S treatment at elevated temperatures (600 °C and 800 °C). Carbon dioxide and methane uptake at atmospheric (0.1 MPa) and high pressure (4 MPa) adsorption results depicted the microporous structure as the main structural parameter defining the adsorption performance. Nevertheless, the surface chemistry also influenced the adsorption properties. Figure 12 shows the normalized uptake (mg/cm^3) by the micropore volume (most influential textural parameter) for the different samples evaluated as a function of the atomic percentage of sulfur estimated from the XPS data. In this figure, a certain positive effect of the surface chemistry is observed, for oxidized samples, most probably due to the synergic effect between sulfur and oxygen functionalities. Overall, the cumulative effect of improved textural and chemical properties resulted in up to 27% higher CO_2 uptake at 4 MPa (oxidation + H_2S treatment at 800 °C).

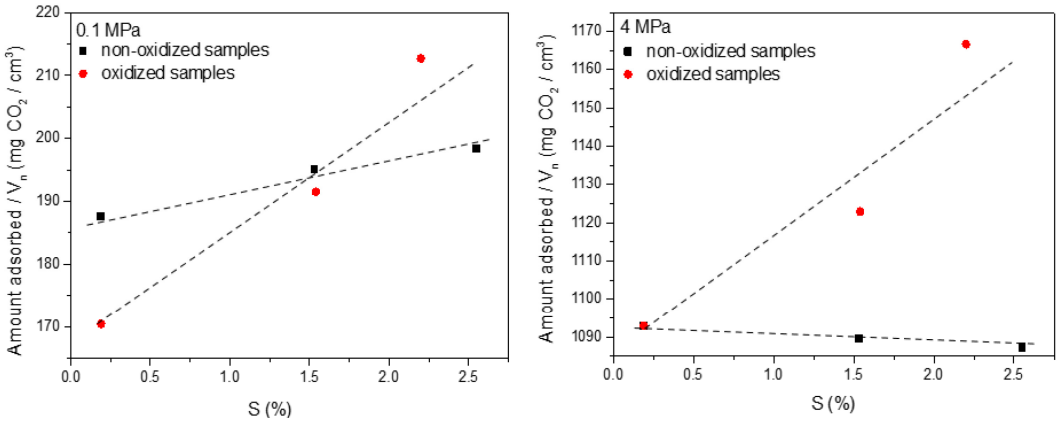

Figure 12. Correlation between the amount of sulfur functional groups on the carbon surface (deduced from the XPS results) and the excess amount adsorbed for CO_2 at atmospheric and high pressure after normalization using the narrow micropore volume (source: [145]).

In order to increase CH_4/CO_2 selectivity, Peredo et al. carried out the surface modification of a commercial AC by a two-step process: oxidative thermal treatment followed by ammonia modification [145]. Their results show that the modification compromised the textural properties of the AC, which significantly lowered the adsorption capacity of the modified AC. Nevertheless, a remarkable increase in the experimental selectivity was found upon surface modification, achieving a selectivity of 9.1 at 1 MPa and 129 at 2.17 MPa; these values are comparable to highly selective materials such as MOFs and zeolites. The governing factor behind the increased selectivity was found to be the presence of basic functionalities. The modification was proven to have cyclic stability over ten consecutive adsorption/desorption cycles.

Textural properties can also be modified by treatment of produced activated carbons, i.e., the pyrolysis of activated carbons at temperatures ranging from 773 to 1273 K results in the removal of heterogeneous atoms, leaving a stiff carbon matrix with a narrower pore size distribution consisting of micropores and ultramicropores. The resulting adsorbent, named Carbon Molecular Sieves (CMS), is considered a subrange of AC with interesting gas selectivity properties based on kinetic adsorption [149].

Carbon Molecular Sieves can effectively separate different gas molecules through a sieving process based on the size and kinetic diameter of each probe. They can be tailored to have a narrow pore size distribution that results in kinetically preferential adsorption of CO_2 from CH_4 due to its smaller kinetic diameter (3.3 Å for CO_2 vs. 3.8 Å for CH_4) [150]. Their separation performance is highly influenced by contact time, intraparticle diffusion, mass transfer rates, and adsorbate–adsorbent surface group interaction forces.

Yu et al. studied the effect of fluorination of a commercial CMS on CH_4/CO_2 mixture adsorption at various fluorine (F_2) partial pressures; the added fluorine groups resulted in an overall increase in pore sizes that became more pronounced at higher partial pressures. This in turn enhanced the carbon dioxide adsorption capacity from 1.61 to 2.04 mmol g^{-1} at 298 K, while maintaining a selective adsorption towards this gas, evidenced by a longer breakthrough times during CH_4/CO_2 dynamic adsorption tests [151].

Commercial CMS usually shows lower adsorption capacities than activated carbons (ACs) and zeolites [152]. Nevertheless, their CH_4/CO_2 selectivity is higher, resulting in higher methane yields, i.e., Rainone et al. compared the adsorption properties of the CMS Xintao against two commercial ACs (Carbotech and Desotec). Their findings show that the CMS shows the best compromise between maximum equilibrium CO_2 adsorption capacity, CO_2 breakpoint adsorption capacity (Xintao: 0.37 mmol g^{-1}, Carbotech: 0.31 mmol g^{-1}, and Desotec: 0.95 mmol g^{-1}), kinetic parameters, and CH_4/CO_2 selectivity (Xintao: 12.71, Carbotech: 15.07, and Desotec: 2.89). The study also highlights the complete regenerability capacity of the CMS after 10 consecutive adsorption/desorption cycles. CMS has also been studied as an interesting alternative for membrane-based biogas upgrading due to its high thermal and chemical stability [153].

Section Summary

The post-synthesis modification of activated carbons is a promising approach to enhance the CO_2 adsorption performance for biogas upgrading. These techniques aim to improve key properties such as selectivity and adsorption capacity by introducing or modifying surface functional groups after the initial activation process. Among the most common methods, amine impregnation—particularly with TEPA and MEA—has shown significant improvements in CO_2 capture, especially under low-pressure conditions. Other modifications proposed in the literature include oxidation treatments and functionalization with metal oxides or salts and sulfur doping. Nevertheless, the post-synthesis modification often involves a loss of textural parameters or decreased regeneration performance. Despite these limitations, post-synthesis modifications offer a practical pathway to tailor activated carbons for specific biogas compositions and operating conditions, improving their applicability in upgrading processes.

5. Additional Factors That Influence the Adsorption Performance of ACs

Gil et al. also emphasized the importance of volumetric uptake experimental determinations for gas separation processes such as biogas upgrading by comparing two ACs produced from Novolac phenol formaldehyde resins, an AC obtained from the same residue mixed with olive stone, and two commercial ACs [154]. The authors determined important deviations between the CO_2 adsorption capacity from the CH_4/CO_2 gas mixtures on a mass basis than the tendencies observed for volumetric uptakes under the same

conditions for the set of adsorbents; thus, the AC that showed higher carbon dioxide capacity was not determined to be the overall better option when plant optimization parameters are added into consideration. This assertion has important implications in the optimization of adsorption-based systems, as analyzing volumetric uptake becomes highly relevant for reducing equipment sizes in an industrial application and lowering the cost of the adsorbent inventory. In addition, among all the adsorbents, the activated carbon that showed better potential for biogas upgrading industrial application was found to be the one obtained from the mixture of olive stones and phenol formaldehyde resins. This result is also relevant in terms of new research on the production of ACs from mixtures of locally available organic residues.

Prauchner et al. also highlighted the importance of measuring CO_2 uptake both on a gravimetric and volumetric basis [135]. Their results show that upon comparison of ACs produced from the same precursor by different activation methods and conditions, important deviations from the CO_2 uptake can be found when calculated on a gravimetric versus volumetric basis (see Figure 13). In particular, higher gravimetric uptakes were related to higher ultramicropore volume, while volumetric adsorption was found to also be influenced by the AC skeleton density.

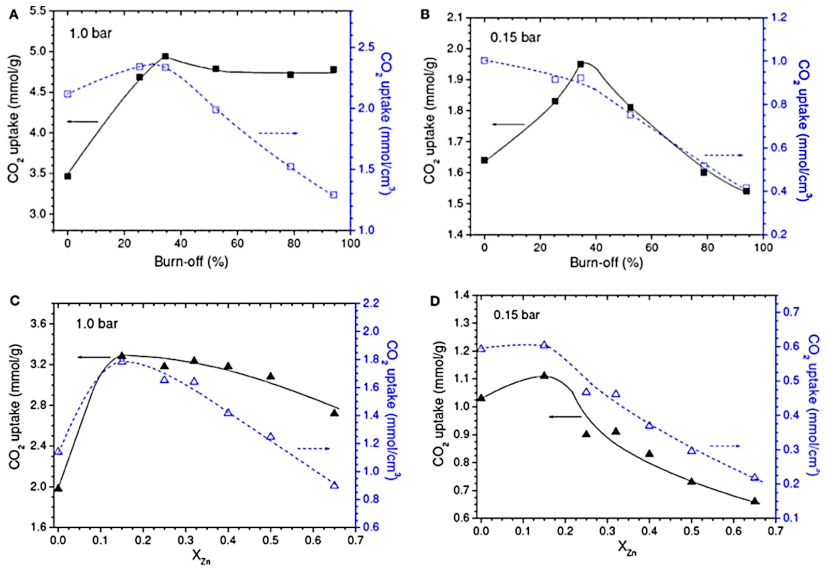

Figure 13. Gravimetric and volumetric CO_2 uptakes as a function of the burn-off during physical activation with CO_2, at (**A**) 1.0 and (**B**) 0.15 bar, and as a function of the chemical loading during chemical activation with $ZnCl_2$ at (**C**) 1.0 and (**D**) 0.15 bar (source: [135]).

As Rios et al. discussed in their work, another factor to take into consideration for the design and optimization of industrial gas separation processes is the experimental CH_4/CO_2 adsorption equilibrium behavior [155]. As the authors discuss, the study of the CH_4/CO_2 mixture adsorption allows for the determination of the role of the adsorbent properties on the adsorption process when competition factors are involved. By studying the adsorption of carbon dioxide and methane from CH_4/CO_2 mixtures with different compositions by a commercial activated carbon. The total adsorbed amount of carbon dioxide increased along with CO_2 composition, indicating competition for adsorption sites that favored carbon dioxide adsorption due to its higher critical temperature of 304 K vs. 190 K for methane, as well as by its higher polarizability. The best selectivity values were obtained for low pressure (0.1 MPa) for a nearly equimolar mixture, indicating that the working pressure also highly impacts the adsorption behavior of mixtures.

In this context, Zhang et al. characterized the pure gas and CH_4/CO_2 mixture adsorption on a granular activated carbon (GAC) via air oxidation, carbonization, and physical

activation using anthracite as the raw material [156]. The effect of the adsorption temperature (278, 298, and 318 K), as well as the CO_2 initial concentration in the gas phase (30%, 50%, and 70%), was analyzed. As the adsorption temperature was increased, the pure gas adsorption capacity of both methane and carbon dioxide was lowered, and the CO_2/CH_4 separation coefficient, an indicator of the adsorption selectivity, was also slightly lowered but remained around 3, which is suitable for industrial applications. The obtained binary gas mixture adsorption isotherms showed that carbon dioxide adsorption capacity is always greater than that of methane even when methane content of the inlet gas was significantly higher (CH_4/CO_2 70/30% *v*/*v*) and in accordance with the previously reviewed work, higher CO_2 content in the initial gas mixture resulted in higher carbon dioxide uptake.

Similarly, Balys et al. [52] studied the gas separation process with the purpose of enriching biogas in biomethane by a biomass-based AC produced from coconut shell, a by-product of waste rubber tire pyrolysis char (RPC), and a commercial carbon molecular sieve (CMS). To this end, they conducted breakthrough experiments at 293 K using two mixtures: (a) 75% CH_4 and 25% CO_2 and (b) 25% CH_4 and 75% CO_2. From the obtained breakthrough curves (see Figure 14), a higher CO_2 adsorption is noted for the carbon dioxide-rich mixture for all of the samples, explained by a higher partial pressure of CO_2 in the gas phase. The CO_2 adsorption capacity for the methane-rich mixture (75% CH_4) followed the order CMS > AC > RPC, while for the carbon-dioxide-rich mixture (75% CO_2), the uptake trend was AC > CMS > RPC. Furthermore, for the methane-rich, the three samples allowed a purity of CH_4 in the outlet stream above 95 vol%, which is the typical minimum purity level requested to meet natural gas grid quality. On the other hand, only the ACs produced a methane stream with the required purity for the CO_2-rich inlet, evidencing the importance of measuring not only the adsorption capacities of the adsorbent material but also its dynamic performance under different operating conditions.

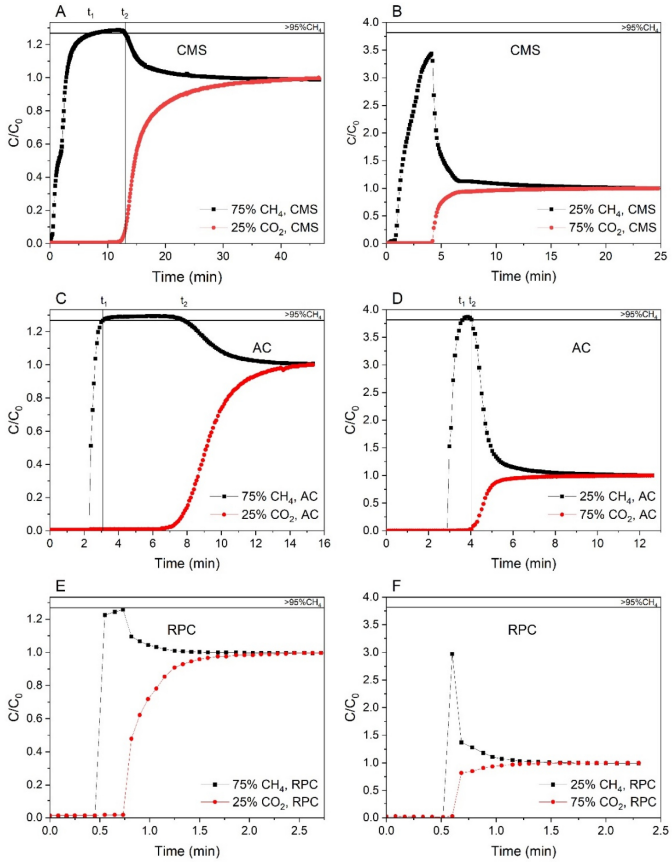

Figure 14. Breakthrough curves for the CMS (**A**,**B**), ACs (**C**,**D**), and RPC (**E**,**F**) samples of the methane-rich mixture and the carbon dioxide-rich mixture, respectively, at 1 bar and 293 K (source: [52]).

CO_2 and CH_4 pure gas adsorption tests provide valuable information in terms of the adsorption capacity of the adsorbent. The use of predictive models to determine the gas mixture adsorption behavior dominates over real mixture adsorption experiments. In order to obtain more reliable data on the competitive factors and the influence of both textural and chemical properties of the adsorbent to selectively adsorb one component, it is highly recommended to evaluate the adsorption performance under biogas upgrading industrial-like conditions, both on an equilibrium and dynamic basis [146]. To this day, CH_4/CO_2 multicomponent adsorption isotherms over different pressures, temperatures, and gas feed compositions remain limited, and as the articles reviewed in the present section demonstrate, the conditions at which adsorption takes place are highly influential on the adsorption behavior.

Furthermore, the ability of the adsorbent material to be easily regenerated and to withstand several adsorption–desorption cycles without compromising its chemical/structural stability is key for the economic feasibility of an adsorption-based system. Additionally, materials with low energy regeneration costs are preferred. The stability of an adsorbent can be assessed by evaluating the adsorption isotherms through several adsorption–desorption cycles mimicking industrial temperature and pressure conditions [152].

Activated carbons tend to have lower heats of adsorption than those of other adsorbent materials such as MOF and zeolites. Typical isosteric heats of adsorption of ACs range from 15 to 25 KJ per mol; thus, regeneration during the desorption phase of ACs has low energy requirements. Chinea et al. evaluated the methane enrichment of biogas by adsorption of gas molecules in a pilot-scale biogas upgrading system [157]. By comparing a commercial activated carbon with calcium hydroxide, they concluded that the AC allows lower recovered gas purity (87% vs. 99% methane purity). Nevertheless, due to the ease of regeneration and the low cost of the adsorbent, AC adsorption-based biogas upgrading showed to have comparable estimated costs to other technologies available on the market, while calcium hydroxide showed to not be cost-effective due to the complexity of the regenerative process.

In order to evaluate and compare adsorbents based on available adsorption data for an initial selection of adsorbents for further tests, some authors have proposed the use of Adsorption Performance Indicators (API) that encompasses several relevant properties, thus allowing a comparison method. In this context, Álvarez-Gutiérrez et al. [123] proposed an API for biomass-based ACs that balances selectivity, $S_{1/2}$, working capacity, WC, and isosteric heat of adsorption, Q_{st}, (Equation (2)):

$$\mathrm{API} = \frac{(S_{1/2}-1)^{A} WC_1^{B}}{|Q_{st,1}|^{C}} \quad (2)$$

In this equation, subscript 1 indicates CO_2. The isosteric heat of adsorption of the strong adsorbate, $Q_{st,1}$ is in the denominator because the heat generated during adsorption is detrimental to the performance of the process. A, B, and C have a default value of 1, and they can be redefined according to the parameter considered more relevant to the study. In the work, API was evaluated for two ACs produced by physical activation with CO_2 (CS-CO_2) and H_2O (CS-H_2O), respectively. The obtained results, shown in Table 6, show that according to the API values, the CO_2 activated carbon shows overall performance upon consideration of the energy needed for regeneration (Q_{st}), purity of the outlet and methane slip (S), and productivity (WC).

Table 6. Selectivity, CO_2 working capacity, average CO_2 adsorption enthalpy, API indicator, and selection parameter S, for the CS adsorbents (Source: [123]).

Sample	$S_{CO2/CH4}$	WC, CO_2 (mol kg^{-1})	Q_{st}, CO_2 (KJ mol^{-1})	API
CS-CO_2	4.35	2.83	21.15	1.27
CS-H_2O	4.39	2.60	23.03	1.00

Abou-Alfa et al. [11] employed a novel Approximate Adsorption Performance Indicator (AAPI) for evaluating the adsorbent performance of one activated biochar produced at 900 °C (Bamboo-A-900) and two pyrolyzed biochars at 500 °C (Bamboo-500) and 700 °C (Bamboo-700), all of them prepared from bamboo. AAPI is based on pure gas adsorption isotherms and takes into account the approximate selectivity (AS), adsorption capacity of CO_2 (n^{B}_{adsCO2}), and heat of adsorption of CO_2 ($Q_{st,1}$), expressed as follows (Equation (3)):

$$AAPI = \frac{(AS_{1/2}-1)^{A} n^{B}_{adsCO2}}{|Q_{st,1}|^{C}} \quad (3)$$

The obtained AAPI results show that the choice of the adsorbent varies with the pressure (see Figure 15), i.e., at low pressure, bamboo-500 showed the highest AAPI values due to a its high AS, the lowest heat of CO_2 adsorption, and the lowest CH_4 adsorption capacity. However, at pressures above 0.12 MPa, AAPI values depict Bamboo-A-900 as the most effective adsorbent, attributed to more developed textural properties and the presence of oxygen surface functionalities.

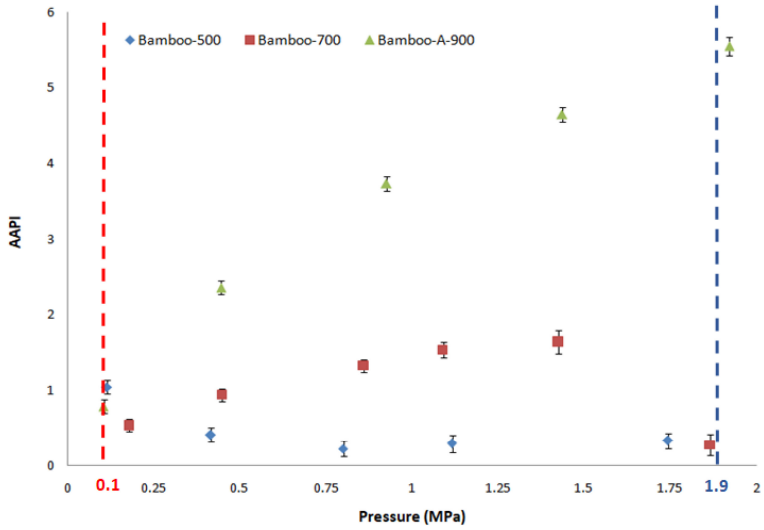

Figure 15. AAPI values of the bamboo family at 303 K versus pressure. Uncertainty calculated using the propagation of errors formula (source: [11]).

The reviewed literature on the use of performance indicators for the evaluation of ACs highlights the importance of incorporating gas interactions and competitive adsorption factors when comparing adsorbent materials for CH_4/CO_2 adsorption and separation since assessing the adsorption behavior purely on the adsorption of pure gases does not take into consideration all the parameters involved for the industrial application of the adsorbent. Furthermore, for a particular AC, its performance is highly dependent on the working conditions (temperature and pressure).

5.1. Comparison of ACs with Other Adsorbent Materials for Biogas Upgrading

Several porous materials have been evaluated for biogas upgrading, including zeolites, metal organic frameworks (MOF), and carbonaceous adsorbents such as ACs and

CMS. One of the main challenges for the implementation of activated carbons for biogas upgrading is their low selectivity compared with zeolites and Metal Organic Frameworks (Table 7). In this context, surface modification of ACs has become an active research field that has shown promising results for significantly increasing selectivity [146].

Table 7. Comparison of CH_4/CO_2 Selectivity (1 MPa) and Maximum Selectivity of Different Adsorbents. * Ideal selectivity values.

Sample	Type	Selectivity (1 MPa, T = 303 K)	Max. Selectivity	Mol (%) CO_2	T (K)	Ref
NaX *	Zeolite	76 (0.1 MPa)		50	303	[21]
CaX *	Zeolite	22 (0.1 MPa)		50	303	[21]
CaA *	Zeolite	44 (0.1 MPa)		50	303	[21]
4A *	Zeolite		200	50	293	[158]
5A	Zeolite		256.47	50		[159]
CMS CT-350 CarboTech	CMS	28.4		20		[154]
CMS-240 (Xintao)	CMS	34.9		10		[154]
P-AC	AC	38		50		[20]
CNR-115-ox-am	AC		129	50	303	[146]
CNR	AC	1.8		50	303	[160]
GAC 1240	AC	2.7		50	303	[160]
AC WV1050 *	AC	5.22	8.7	47	293	[156]
Norit R1 *	AC	2.7		42	298	[161]
HKUST-1-MOF *	MOF		6	50	293	[158]
MOF-5 *	MOF		15.53	50	298	[159]
MOF-177 *	MOF		4.43	50	298	[159]

On the other hand, as discussed throughout the present review, ACs have properties that make them excellent candidates for CO_2 capture and separation, such as tunable textural properties, cyclic and thermal stability, low regeneration energy, and high adsorption capacities (see Table 8). In contrast, Zeolites are recognized for having high CH_4/CO_2 selectivity values; their main drawback is their high sensitivity to the presence of moisture. Finally, MOFs have poor thermal and hydrolytic stability as well as high production costs [162,163].

Table 8. Main properties of adsorbents for CO_2/CH_4 separation (Source: [20]).

	AC	MOF	Zeolite
CO_2 adsorption capacity	High	Medium	High
CO_2/CH_4 selectivity	Low	Medium	High
PSA regeneration	Feasible	Not documented	Feasible ($P < P_{atm}$)
Cost (USD kg^{-1})	0.6–2.4	10.0–70.0	0.6–5.0
Other considerations	Sustainable precursors	Low thermal and hydrolytic stability	High CO_2 adsorption heat

5.2. Section Summary

Additional factors significantly affect the performance of activated carbons (ACs) in biogas upgrading processes, beyond their textural and chemical properties. Operating

temperature, pressure, and gas inlet composition greatly influence the adsorption capacity and selectivity of the adsorbent. The literature review shows a gap in equilibrium and dynamic adsorption experiments under real biogas-like conditions. Other relevant factors for the industrial transferability of the adsorbent are the carbon dioxide volumetric uptake, ease of adsorbent regeneration, and thermal stability. The use of Adsorption Performance Indicators (APIs) allows the comparison of different adsorbents on a multifactor basis. ACs remain competitive due to their availability, scalability, and lower environmental and economic costs.

6. Implementation Barriers and Challenges

While activated carbons offer important advantages in biogas upgrading, several challenges must still be addressed. For instance, the cost and availability of raw materials for producing activated carbons could play a critical role [164]. In this context, the use of locally sourced waste from other processes can be highly advantageous [165]. Additionally, the capital cost required for the installation and adaptation of biogas production and upgrading systems could also represent a significant hurdle for projects, especially if they are of smaller scales [166]. Similarly, of utmost importance are any economic incentives that could be available locally, as they can considerably improve the financial viability of upgrading operations [164]. Furthermore, costs associated with production could be considerable (for example, those associated with chemical activation), while regeneration of biowaste-derived activated carbons used in continuous flow systems is under-researched.

Two of the main environmental benefits of using activated carbons in biogas upgrading are CO_2 separation and capture, as well as their potential contribution to circular economy schemes when produced from locally sourced biowastes. Nevertheless, they also face challenges that must be improved on. As mentioned earlier, both physical and chemical activation processes involve significant amounts of energy, which, if sourced from non-renewable sources, will contribute to climate change and air quality problems. Likewise, if the substrates used are obtained from non-renewable sources, their environmental footprint may be of concern [5]. Figure 16 summarizes the main environmental impacts and challenges of activated carbons both during production and in use for biogas upgrading.

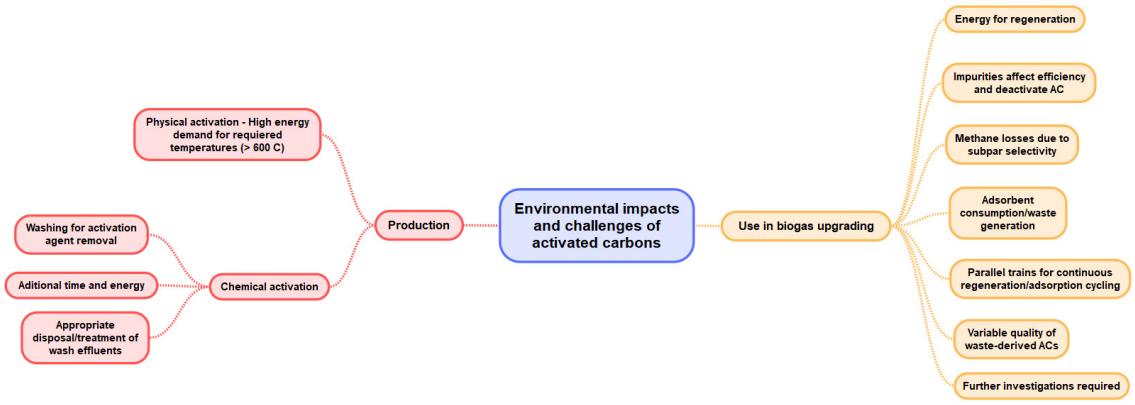

Figure 16. Environmental impacts and challenges of activated carbons in their production and use in biogas upgrading (authors◎elaboration with data from [5–7,11,16,49].

Finally, it is clear that activated carbons show many promises in biogas upgrading and that they exhibit great relevance within adsorption-based technologies. Their eco-friendliness, low energy needs, safe operation, removal efficiency, and flexible design make them very attractive. Nevertheless, there are also key areas where these materials must be further explored and improved. These include enhancing CO_2 adsorption

capacity and selectivity, (particularly through chemical activation methods), addressing the energy requirements of regeneration through the study of its kinetics and thermodynamics, improving their performance in real biogas conditions taking into account impurities (i.e., H_2S, water vapor), and shaping the powders obtained into useful presentations with low pressure drops when used for instance in packed columns. Furthermore, improving production methods without negative impacts on the sustainability of biowaste-derived ACs must also be further researched. Likewise, life cycle assessments including all substances involved as well as all operational parameters require further consideration so as to reduce capital and operational costs [5,11,49,62].

7. Conclusions

The present work explores the potential of activated carbons for biogas upgrading, depicting several techno-economic advantages, including a high surface area of up to 3000 $m^2\ g^{-1}$ for commercial activated carbons and up to 2000 $m^2\ g^{-1}$ for biomass-based AC. In addition, their porosity can be tuned in order to obtain higher CO_2 adsorption capacities. In this context, maximum adsorption values of up to 10.9 mol kg^{-1} are reported in the literature. Furthermore, due to their low CO_2 adsorption heat, typically ranging from 20 to 30 kJ mol^{-1}, they have low regeneration energy requirements. CH_4/CO_2 breakthrough adsorption experiments indicate that methane purity levels of up to 95% can be obtained using ACs as the adsorbent material through several adsorption–desorption cycles. Another important advantage is that they can be produced from sustainable sources such as agricultural and food wastes, and more recently, from plastic waste. The adsorption properties are shown to be highly influenced by the substrate choice and the activation process. The suitability of ACs requires the systematic exploration of how activation parameters (such as activation agent, activation agent ratio, flow rate, temperature) influence both the textural and chemical properties of the resulting adsorbent and, in turn, their effect on the adsorption behavior. Overall, the presence of developed ultramicroporosity has been found to be the most influential parameter for carbon dioxide uptake on ACs; nevertheless, the presence of wider pores is also required to allow the diffusion of the gas molecules into the adsorbent structure to reach the narrower pores. Additionally, the presence of basic surface groups can help enhance the selectivity towards carbon dioxide; selectivity values of up to 129 for modified AC are described in the literature. The addition of surface basic functionalities can result from choosing the right activation agent, or alternatively, can be produced by post-synthesis treatment of AC. Finally, although many promising carbonaceous adsorbents demonstrate favorable performance under laboratory conditions, they still face significant challenges in real-world biogas upgrading applications. Much of the ongoing research is based on equilibrium conditions and pure gas adsorption predictions. The presented literature also highlights the key relevance of taking into consideration industrial operation parameters such as dynamic performance, cyclability, volumetric volume uptake, adsorption, and regeneration behavior under pressure- or temperature-swing conditions and variable inlet gas compositions.

Author Contributions: Conceptualization, D.P.-M., A.B., and D.B.; writing—original draft preparation, D.P.-M. and A.B.; investigation, D.P.-M., A.B., C.H. and D.B.; data curation, D.P.-M.; proofreading, D.P.-M., A.B., C.H. and D.B.; writing—review and editing, D.P.-M., A.B., C.H. and D.B.; supervision, D.B. All authors have read and agreed to the published version of the manuscript.

Funding: This research received no external funding.

Conflicts of Interest: The authors declare no conflict of interest.

References

1. UN. Sustainable Development Goals. 2015. Available online: https://sdgs.un.org/ (accessed on 1 April 2025).
2. IEA. Renewables 2024. Paris, 2024. Available online: https://www.iea.org/reports/renewables-2024 (accessed on 1 April 2025).
3. IEA. Outlook for Biogas and Biomethane: Prospects for Organic Growth; Paris, 2020. https://www.iea.org/reports/outlook-for-biogas-and-biomethane-prospects-for-organic-growth (accessed on 1 April 2025).
4. Mihi, M.; Ouhammou, B.; Aggour, M.; Daouchi, B.; Naaim, S.; El Mers, E.M.; Kousksou, T. Modeling and forecasting biogas production from anaerobic digestion process for sustainable resource energy recovery. *Heliyon* **2024**, *10*, e38472. https://doi.org/10.1016/j.heliyon.2024.e38472.
5. Bernardo, M.; Lapa, N.; Fonseca, I.; Esteves, I.A.A.C. Biomass Valorization to Produce Porous Carbons: Applications in CO_2 Capture and Biogas Upgrading to Biomethane—A Mini-Review. *Front. Energy Res.* **2021**, *9*, 625188. https://doi.org/10.3389/fenrg.2021.625188.
6. Comesaña-Gándara, B.; García-Depraect, O.; Santos-Beneit, F.; Bordel, S.; Lebrero, R.; Muñoz, R. Recent trends and advances in biogas upgrading and methanotrophs-based valorization. *Chem. Eng. J. Adv.* **2022**, *11*, 100325. https://doi.org/10.1016/j.ceja.2022.100325.
7. López, A.F.; Rodríguez, T.L.; Abdolmaleki, S.F.; Martínez, M.G.; Bugallo, P.M.B. From Biogas to Biomethane: An In-Depth Review of Upgrading Technologies That Enhance Sustainability and Reduce Greenhouse Gas Emissions. *Appl. Sci.* **2024**, *14*, 2342. https://doi.org/10.3390/app14062342.
8. Mohammadpour, H.; Cheng, K.Y.; Pivrikas, A.; Ho, G. A review of biogas upgrading technologies: Key emphasis on electrochemical systems. *Water Sci. Technol.* **2025**, *91*, 93–116. https://doi.org/10.2166/wst.2024.394.
9. Sher, F.; Smječanin, N.; Hrnjić, H.; Karadža, A.; Omanović, R.; Šehović, E.; Sulejmanović, J. Emerging technologies for biogas production: A critical review on recent progress, challenges and future perspectives. *Process Saf. Environ. Prot.* **2024**, *188*, 834–859. https://doi.org/10.1016/j.psep.2024.05.138.
10. Tomczak, W.; Gryta, M.; Daniluk, M.; Żak, S. Biogas Upgrading Using a Single-Membrane System: A Review. *Membranes* **2024**, *14*, 80. https://doi.org/10.3390/membranes14040080.
11. Alfa, K.A.; Saleh, N.A.; Beda, A.; Ghimbeu, C.M.; Dushime, G.I.; Marias, F.; Moynault, L.; Platel, V.; Hort, C. Approximate Adsorption Performance Indicator in Evaluating Sustainable Bamboo-Derived Adsorbents for Biogas Upgrading. *Sustainability* **2025**, *17*, 1445. https://doi.org/10.3390/su17041445.
12. Thrän, D.; Adetona, A.; Borchers, M.; Cyffka, K.-F.; Daniel-Gromke, J.; Oehmichen, K. Potential contribution of biogas to net zero energy systems–A comparative study of Canada and Germany. *Biomass Bioenergy* **2025**, *193*, 107561. https://doi.org/10.1016/j.biombioe.2024.107561.
13. Lawson, N.; Alvarado-Morales, M.; Tsapekos, P.; Angelidaki, I. Techno-economic assessment of biological biogas upgrading based on danish biogas plants. *Energies* **2021**, *14*, 8252. https://doi.org/10.3390/en14248252.
14. Angelidaki, I.; Xie, L.; Luo, G.; Zhang, Y.; Oechsner, H.; Lemmer, A.; Munoz, R.; Kougias, P.G. Biogas upgrading: Current and emerging technologies. In *Biomass, Biofuels, Biochemicals: Biofuels: Alternative Feedstocks and Conversion Processes for the Production of Liquid and Gaseous Biofuels*; Academic Press: Cambridge, MA, USA, 2019; pp. 817–843. https://doi.org/10.1016/B978-0-12-816856-1.00033-6.
15. Golmakani, A.; Nabavi, S.A.; Wadi, B.; Manovic, V. Advances, challenges, and perspectives of biogas cleaning, upgrading, and utilisation. *Fuel* **2022**, *317*, 123085. https://doi.org/10.1016/j.fuel.2021.123085.
16. Kazimierowicz, J.; Dębowski, M.; Zieliński, M. Innovative Method for Biomethane Production Based on a Closed Cycle of Biogas Upgrading and Organic Substrate Pretreatment—Technical, Economic, and Technological Fundamentals. *Energies* **2025**, *18*, 1033. https://doi.org/10.3390/en18051033.
17. Khan, I.U.; Othman, M.H.D.; Hashim, H.; Matsuura, T.; Ismail, A.F.; Rezaei-DashtArzhandi, M.; Wan Azelee, I. Biogas as a renewable energy fuel–A review of biogas upgrading, utilisation and storage. *Energy Convers. Manag.* **2017**, *150*, 277–294. https://doi.org/10.1016/j.enconman.2017.08.035.
18. Yang, M.; Baral, N.R.; Anastasopoulou, A.; Breunig, H.M.; Scown, C.D. Cost and Life-Cycle Greenhouse Gas Implications of Integrating Biogas Upgrading and Carbon Capture Technologies in Cellulosic Biorefineries. *Environ. Sci. Technol.* **2020**, *54*, 12810–12819. https://doi.org/10.1021/acs.est.0c02816.
19. Boer, D.G.; van de Bovenkamp, H.H.; Langerak, J.; Bakker, B.; Pescarmona, P.P. Evaluation of binderless LTA and SAPO-34 beads as CO_2 adsorbents for biogas upgrading in a vacuum pressure swing adsorption setup. *Energy Adv.* **2024**, *3*, 1581–1593. https://doi.org/10.1039/D4YA00007B.

20. Paz, L.; Gentil, S.; Fierro, V.; Celzard, A. Assessing the performance of adsorbents for CO_2/CH_4 separation in pressure swing adsorption units: A review. *J. Environ. Chem. Eng.* **2024**, *12*, 114870. https://doi.org/10.1016/j.jece.2024.114870.
21. Li, Y.; Yi, H.; Tang, X.; Li, F.; Yuan, Q. Adsorption separation of CO_2/CH_4gas mixture on the commercial zeolites at atmospheric pressure. *Chem. Eng. J.* **2013**, *229*, 50–56. https://doi.org/10.1016/j.cej.2013.05.101.
22. Kapoor, R.; Subbarao, P.M.V.; Vijay, V.K.; Shah, G.; Sahota, S.; Singh, D.; Verma, M. Factors affecting methane loss from a water scrubbing based biogas upgrading system. *Appl. Energy* **2017**, *208*, 1379–1388. https://doi.org/10.1016/j.apenergy.2017.09.017.
23. Paolini, V.; Tratzi, P.; Torre, M.; Tomassetti, L.; Segreto, M.; Petracchini, F. Water scrubbing for biogas upgrading: Developments and innovations. In *Emerging Technologies and Biological Systems for Biogas Upgrading*; Elsevier: Amsterdam, The Netherlands, 2021; pp. 57–71. https://doi.org/10.1016/B978-0-12-822808-1.00001-5.
24. Cuimei, B.; Wei, G.; Chao, T.; Jun, L.; Xiaohua, L. Dynamic Control Design and Simulation of Biogas Pressurized Water Scrubbing Process. *IFAC-PapersOnLine* **2018**, *51*, 560–565. https://doi.org/10.1016/j.ifacol.2018.09.365.
25. Jabraeelzadeh, A.; Gharehghani, A.; Saray, J.A.; Andwari, A.M.; Borhani, T.N. Techno-economic analysis of biogas upgrading through amine scrubbing: A comparative study of different single amines. *Fuel* **2025**, *381*, 133662. https://doi.org/10.1016/j.fuel.2024.133662.
26. Capra, F.; Fettarappa, F.; Magli, F.; Gatti, M.; Martelli, E. Biogas upgrading by amine scrubbing: Solvent comparison between MDEA and MDEA/MEA blend. *Energy Procedia* **2018**, *148*, 970–977. https://doi.org/10.1016/j.egypro.2018.08.065.
27. Wang, Y.; Hu, X.; Guo, T.; Tian, W.; Hao, J.; Guo, Q. The competitive adsorption mechanism of CO_2, H_2O and O_2 on a solid amine adsorbent. *Chem. Eng. J.* **2021**, *416*, 129007. https://doi.org/10.1016/j.cej.2021.129007.
28. Gkotsis, P.; Kougias, P.; Mitrakas, M.; Zouboulis, A. Biogas upgrading technologies–Recent advances in membrane-based processes. *Int. J. Hydrogen Energy* **2023**, *48*, 3965–3993. https://doi.org/10.1016/j.ijhydene.2022.10.228.
29. Nishimura, A.; Takada, T.; Ohata, S.; Kolhe, M.L. Biogas Dry Reforming for Hydrogen through Membrane Reactor Utilizing Negative Pressure. *Fuels* **2021**, *2*, 194–209. https://doi.org/10.3390/fuels2020012.
30. Micale, C. Bio-methane generation from biogas upgrading by semi-permeable membranes: An experimental, numerical and economic analysis. *Energy Procedia* **2015**, *82*, 971–977. https://doi.org/10.1016/j.egypro.2015.11.854.
31. Naquash, A.; Qyyum, M.A.; Haider, J.; Bokhari, A.; Lim, H.; Lee, M. State-of-the-art assessment of cryogenic technologies for biogas upgrading: Energy, economic, and environmental perspectives. *Renew. Sustain. Energy Rev.* **2022**, *154*, 111826. https://doi.org/10.1016/j.rser.2021.111826.
32. Song, C.; Fan, Z.; Li, R.; Liu, Q.; Kitamura, Y. Efficient biogas upgrading by a novel membrane-cryogenic hybrid process: Experiment and simulation study. *J. Membr. Sci.* **2018**, *565*, 194–202. https://doi.org/10.1016/j.memsci.2018.08.027.
33. Pellegrini, L.A.; De Guido, G.; Langé, S. Biogas to liquefied biomethane via cryogenic upgrading technologies. *Renew. Energy* **2018**, *124*, 75–83. https://doi.org/10.1016/j.renene.2017.08.007.
34. Biswas, R.; Ahmadi, V.; Ummethala, R.; Mozumder, M.S.I.; Aryal, N. Recent advances in electrochemical carbon dioxide reduction strategies in biogas upgrading and biomethane production. *Chem. Eng. J. Adv.* **2025**, *22*, 100722. https://doi.org/10.1016/j.ceja.2025.100722.
35. Pasternak, G. Electrochemical approach for biogas upgrading. In *Emerging Technologies and Biological Systems for Biogas Upgrading*; Elsevier: Amsterdam, The Netherlands, 2021; pp. 223–254. https://doi.org/10.1016/B978-0-12-822808-1.00009-X.
36. Ray, S.; Kuppam, C.; Pandit, S.; Kumar, P. Biogas Upgrading by Hydrogenotrophic Methanogens: An Overview. *Waste Biomass Valorization* **2023**, *14*, 537–552. https://doi.org/10.1007/s12649-022-01888-6.
37. Zhang, L.; Kuroki, A.; Tong, Y.W. A Mini-Review on In situ Biogas Upgrading Technologies via Enhanced Hydrogenotrophic Methanogenesis to Improve the Quality of Biogas From Anaerobic Digesters. *Front. Energy Res.* **2020**, *8*, 69. https://doi.org/10.3389/fenrg.2020.00069.
38. Venkiteshwaran, K.; Xie, T.; Seib, M.; Tale, V.P.; Zitomer, D. Anaerobic digester biogas upgrading using microalgae. In *Integrated Wastewater Management and Valorization Using Algal Cultures*; Elsevier: Amsterdam, The Netherlands, 2022; pp. 183–214. https://doi.org/10.1016/B978-0-323-85859-5.00004-X.
39. Kikuchi, Y.; Kanai, D.; Sugiyama, K.; Fujii, K. Biogas Upgrading by Wild Alkaliphilic Microalgae and the Application Potential of Their Biomass in the Carbon Capture and Utilization Technology. *Fermentation* **2024**, *10*, 134. https://doi.org/10.3390/fermentation10030134.
40. Di Profio, P.; Ciulla, M.; Di Giacomo, S.; Barbacane, N.; Wolicki, R.D.; Fontana, A.; Moffa, S.; Pilato, S.; Siani, G. Emerging green strategies for biogas upgrading through CO_2 capture: From unconventional organic solvents to clathrate and semi-clathrate hydrates. *J. Mol. Liq.* **2023**, *391*, 123196. https://doi.org/10.1016/j.molliq.2023.123196.

41. Moghaddam, E.A.; Larsolle, A.; Tidåker, P.; Nordberg, Å. Gas Hydrates as a Means for Biogas and Biomethane Distribution. *Front. Energy Res*. **2021**, *9*, 568879. https://doi.org/10.3389/fenrg.2021.568879.
42. Gallego-Fernández, L.M.; Portillo, E.; Borrero, F.V.; Navarrete, B.; Vilches, L.F. CO_2 capture for biogas upgrading using salts, hydroxides, and waste. In *Circular Economy Processes for CO_2 Capture and Utilization*; Elsevier: Amsterdam, The Netherlands, 2024; pp. 7–24. https://doi.org/10.1016/B978-0-323-95668-0.00005-9.
43. Kida, M.; Fujiwara, R.; Goda, H.; Sakagami, H.; Minami, H. Methane and Carbon Dioxide Separation Characteristics of Quaternary Ammonium Salt Hydrates for Biogas Upgrading under Static Conditions of Gas–Solid Contact. *Energy Fuels* **2023**, *37*, 9197–9206. https://doi.org/10.1021/acs.energyfuels.3c00362.
44. Obileke, K. Sustainability evaluation of current biogas upgrading techniques. In *Innovations in the Global Biogas Industry*; Elsevier: Amsterdam, The Netherlands, 2025; pp. 213–244. https://doi.org/10.1016/B978-0-443-22372-3.00008-X.
45. Galloni, M.; Di Marcoberardino, G. Biogas Upgrading Technology: Conventional Processes and Emerging Solutions Analysis. *Energies* **2024**, *17*, 2907. https://doi.org/10.3390/en17122907.
46. Aktar, K.; Yabar, H.; Mizunoya, T.; Islam, M.M. Application of GIS in Introducing Community-Based Biogas Plants from Dairy Farm Waste: Potential of Renewable Energy for Rural Areas in Bangladesh. *Geomatics* **2024**, *4*, 384–411. https://doi.org/10.3390/geomatics4040021.
47. Godfrey, O.U. Renewable Energy from Agricultural Waste: Biogas Potential for Sustainable Energy Generation in Nigeria's Rural Agricultural Communities. *J. Eng. Res. Rep.* **2024**, *26*, 341–367. https://doi.org/10.9734/jerr/2024/v26i121362.
48. Owusu, P.A.; Borkloe, J.K.; Mahamud, Y. Challenges towards Sustainable Energy as a Substitute for Fossil Fuels for the Case of Municipal Waste Management. *J. Earth Energy Sci. Eng. Technol.* **2024**, *7*, 1–14. https://doi.org/10.25105/jeeset.v7i1.18798.
49. Selim, M.M.; Tounsi, A.; Gomaa, H.; Shenashen, M. Enhancing carbon capture efficiency in biogas upgrading: A comprehensive review on adsorbents and adsorption isotherms. *AIP Adv.* **2024**, *14*, 040703. https://doi.org/10.1063/5.0208686.
50. Kamran, U.; Park, S.J. Chemically modified carbonaceous adsorbents for enhanced CO_2 capture: A review. *J. Clean. Prod.* **2021**, *290*, 125776. https://doi.org/10.1016/j.jclepro.2020.125776.
51. Nie, Z.; Lin, Y.; Jin, X. Research on the theory and application of adsorbed natural gas used in new energy vehicles: A review. *Front. Mech. Eng.* **2016**, *11*, 258–274. https://doi.org/10.1007/s11465-016-0381-2.
52. Bałys, M.; Brodawka, E.; Jodłowski, G.S.; Szczurowski, J.; Wójcik, M. Alternative Materials for the Enrichment of Biogas with Methane. *Materials* **2021**, *14*, 7759. https://doi.org/10.3390/ma14247759.
53. Hosseini, S.S.; Denayer, J.F. Biogas upgrading by adsorption processes: Mathematical modeling, simulation and optimization approach—A review. *J. Environ. Chem. Eng.* **2022**, *10*, 107483. https://doi.org/10.1016/j.jece.2022.107483.
54. Karne, H.; Mahajan, U.; Ketkar, U.; Kohade, A.; Khadilkar, P.; Mishra, A. A review on biogas upgradation systems. *Mater. Today. Proc.* **2023**, *72*, 775–786. https://doi.org/10.1016/j.matpr.2022.09.015.
55. Mrosso, R.; Mecha, A.C.; Kiplagat, J. Carbon Dioxide Removal Using a Novel Adsorbent Derived from Calcined Eggshell Waste for Biogas Upgrading. *S. Afr. J. Chem. Eng.* **2024**, *47*, 150–158. https://doi.org/10.1016/j.sajce.2023.11.007.
56. Liu, J.; Chen, Q.; Qi, P. Upgrading of Biogas to Methane Based on Adsorption. *Processes* **2020**, *8*, 941. https://doi.org/10.3390/pr8080941.
57. Solís, R.R.; Calero, M.; Pereira, L.; Ramírez, S.; Blázquez, G.; Martín-Lara, M.Á. Transforming a mixture of real post-consumer plastic waste into activated carbon for biogas upgrading. *Process Saf. Environ. Prot.* **2024**, *190*, 298–315. https://doi.org/10.1016/j.psep.2024.07.022.
58. Chen, Y.; Yin, H.; Wen, S.; Zhang, W.; Hu, S.; Sun, K.; Jiang, J.; Ji, X. Biogas upgrading using aqueous bamboo-derived activated carbons. *Bioresour. Technol.* **2025**, *419*, 132055. https://doi.org/10.1016/j.biortech.2025.132055.
59. Yadavalli, G.; Lei, H.; Wei, Y.; Zhu, L.; Zhang, X.; Liu, Y.; Yan, D. Carbon dioxide capture using ammonium sulfate surface modified activated biomass carbon. *Biomass Bioenergy* **2017**, *98*, 53–60. https://doi.org/10.1016/j.biombioe.2017.01.015.
60. Shafeeyan, M.S.; Daud, W.M.A.W.; Houshmand, A.; Shamiri, A. A review on surface modification of activated carbon for carbon dioxide adsorption. *J. Anal. Appl. Pyrolysis* **2010**, *89*, 143–151. https://doi.org/10.1016/j.jaap.2010.07.006.
61. Canevesi, R.L.S.; Schaefer, S.; Izquierdo, M.T.; Celzard, A.; Fierro, V. Roles of Surface Chemistry and Texture of Nanoporous Activated Carbons in CO_2 Capture. *ACS Appl. Nano Mater.* **2022**, *5*, 3843–3854. https://doi.org/10.1021/acsanm.1c04474.
62. Gao, X.; Yang, S.; Hu, L.; Cai, S.; Wu, L.; Kawi, S. Carbonaceous materials as adsorbents for CO2 capture: Synthesis and modification. *Carbon Capture Sci. Technol.* **2022**, *3*, 100039. https://doi.org/10.1016/j.ccst.2022.100039.
63. Sosa, J.A.; Laines, J.R.; García, D.S.; Hernández, R.; Zappi, M.; de los Monteros, A.E.E. Activated Carbon: A Review of Residual Precursors, Synthesis Processes, Characterization Techniques, and Applications in the Improvement of Biogas. *Environ. Eng. Res.* **2022**, *28*, 220100. https://doi.org/10.4491/eer.2022.100.

64. Surra, E.; Ribeiro, R.P.P.L.; Santos, T.; Bernardo, M.; Mota, J.P.B.; Lapa, N. Evaluation of activated carbons produced from Maize Cob Waste for adsorption-based CO_2 separation and biogas upgrading. *J. Environ. Chem. Eng.* **2022**, *10*, 107065. https://doi.org/10.1016/j.jece.2021.107065.
65. Bonaccorsi, L.; Fazzino, F.; Fotia, A.; Malara, A.; Pedullà; A.; Calabrò, P.S. Comparison at laboratory scale of different types and configurations of commercial molecular sieves for one-step direct upgrading of biogas produced by anaerobic digestion. *Fuel* **2024**, *365*, 131292. https://doi.org/10.1016/j.fuel.2024.131292.
66. Maulidaturahma, E.; Ariyanto, T.; Lestari, R.A.S.; Purnomo, C.W. Biogas purification by using zeolite packing columns. *AIP Conf. Proc.* **2024**, *3116*, 060001. https://doi.org/10.1063/5.0210352.
67. Jiang, Y.; Ling, J.; Xiao, P.; He, Y.; Zhao, Q.; Chu, Z.; Liu, Y.; Li, Z.; Webley, P.A. Simultaneous biogas purification and CO2capture by vacuum swing adsorption using zeolite NaUSY. *Chem. Eng. J.* **2018**, *334*, 2593–2602. https://doi.org/10.1016/j.cej.2017.11.090.
68. Duma, Z.; Makgwane, P.R.; Masukume, M.; Swartbooi, A.; Rambau, K.; Mehlo, T.; Mavhungu, T. A comprehensive review of metal-organic frameworks sorbents and their mixed-matrix membranes composites for biogas cleaning and CO_2/CH_4 separation. *Mater. Today Sustain.* **2024**, *27*, 100812. https://doi.org/10.1016/j.mtsust.2024.100812.
69. Abd, A.A.; Kim, J.; Jasim, D.J.; Othman, M.R. Production of green methane by carbon dioxide capture from landfill biogas via pressure swing adsorption mediated by MOF ZIF-8. *Energy Convers. Manag.* **2024**, *321*, 119090. https://doi.org/10.1016/j.enconman.2024.119090.
70. Lee, M.S.; Park, M.; Kim, H.Y.; Park, S.J. Effects of Microporosity and Surface Chemistry on Separation Performances of N-Containing Pitch-Based Activated Carbons for CO_2/N_2 Binary Mixture. *Sci. Rep.* **2016**, *6*, 23224. https://doi.org/10.1038/srep23224.
71. Abd, A.A.; Othman, M.R.; Kim, J. A review on application of activated carbons for carbon dioxide capture: Present performance, preparation, and surface modification for further improvement. *Environ. Sci. Pollut. Res.* **2021**, *28*, 43329–43364. https://doi.org/10.1007/s11356-021-15121-9.
72. Wu, Y.-J.; Yang, Y.; Kong, X.-M.; Li, P.; Yu, J.-G.; Ribeiro, A.M.; Rodrigues, A.E. Adsorption of Pure and Binary CO_2, CH_4, and N_2 Gas Components on Activated Carbon Beads. *J. Chem. Eng. Data* **2015**, *60*, 2684–2693. https://doi.org/10.1021/acs.jced.5b00321.
73. Durán, I.; Álvarez-Gutiérrez, N.; Rubiera, F.; Pevida, C. Biogas purification by means of adsorption on pine sawdust-based activated carbon: Impact of water vapor. *Chem. Eng. J.* **2018**, *353*, 197–207. https://doi.org/10.1016/j.cej.2018.07.100.
74. Buczek, B. Methane Recovery from Gaseous Mixtures Using Carbonaceous Adsorbents. *Arch. Min. Sci.* **2016**, *61*, 285–292. https://doi.org/10.1515/amsc-2016-0021.
75. Chen, F.; Zhang, Z.; Yang, Q.; Yang, Y.; Bao, Z.; Ren, Q. Microporous Carbon Adsorbents Prepared by Activating Reagent-Free Pyrolysis for Upgrading Low-Quality Natural Gas. *ACS Sustain. Chem. Eng.* **2020**, *8*, 977–985. https://doi.org/10.1021/acssuschemeng.9b05627.
76. Całus-Makowska, K.; Grosser, A.; Grobelak, A.; Białek, H.; Siedlecka, E. Kinetic study of the simultaneous removal of ibuprofen, carbamazepine, sulfamethoxazole, and diclofenac from water using biochar and activated carbon adsorption, and TiO_2 photocatalysis. *Desalination Water Treat.* **2024**, *320*, 100817. https://doi.org/10.1016/j.dwt.2024.100817.
77. Arenas, L.R.; Le Coustumer, P.; Gentile, S.R.; Zimmermann, S.; Stoll, S. Removal efficiency and adsorption mechanisms of CeO_2 nanoparticles onto granular activated carbon used in drinking water treatment plants. *Sci. Total Environ.* **2023**, *856*, 159261. https://doi.org/10.1016/j.scitotenv.2022.159261.
78. Paparo, R.; Trifuoggi, M.; Uggeri, F.; Nicolais, L.; Russo, V.; Di Serio, M. Intensification of the adsorption process to remove Iopamidol from water using granular activated carbon: Use of Rotating Packed Reactor and ultrasound technique in continuous flow technology. *Chem. Eng. Process. Process Intensif.* **2025**, *209*, 110166. https://doi.org/10.1016/j.cep.2025.110166.
79. Salas, M.A.G.; Mendoza-Castillo, D.I.; Bonilla-Petriciolet, A.; Jiménez-Junca, C. Functionalized activated carbon with whey protein amyloid fibrils for adsorption of arsenic from water. *Environ. Nanotechnol. Monit. Manag.* **2024**, *22*, 100956. https://doi.org/10.1016/j.enmm.2024.100956.
80. Sriprom, P.; Assawasaengrat, P.; Kraijan, P.; Laonork, S.; Rodmee, A.; Manamoongmongkol, K.; Permana, L.; Phumjan, L.; Kerdpiboon, S.; Puttongsiri, T. Activated carbon derived from Mahachanok mango seeds as a potential material to delay the ripening of mangoes. *J. Agric. Food Res.* **2024**, *18*, 101432. https://doi.org/10.1016/j.jafr.2024.101432.
81. Regadera-Macías, A.M.; Morales-Torres, S.; Pastrana-Martínez, L.M.; Maldonado-Hódar, F.J. Optimizing filters of activated carbons obtained from biomass residues for ethylene removal in agro-food industry devices. *Environ. Res.* **2024**, *248*, 118247. https://doi.org/10.1016/j.envres.2024.118247.

82. Priya, D.S.; Kennedy, L.J.; Anand, G.T. Porous activated carbon electrodes derived from Eleusine coracana biowaste in electric double layer capacitors: Nanoarchitectonics and performance. *Results Surf. Interfaces* **2024**, *17*, 100353. https://doi.org/10.1016/j.rsurfi.2024.100353.
83. Dhapola, P.S.; Kumar, S.; Karakoti, M.; Yahya, M.Z.A.; Punetha, V.D.; Pandey, S.; Chowdhury, F.I.; Savilov, S.V.; Singh, P.K. O, N co-doped porous activated carbon from polyvinyl chloride for super capacitors and solar cells application. *Chem. Phys. Impact* **2024**, *9*, 100721. https://doi.org/10.1016/j.chphi.2024.100721.
84. Bandara, T.M.W.J.; Alahakoon, A.M.B.S.; Mellander, B.E.; Albinsson, I. Activated carbon synthesized from Jack wood biochar for high performing biomass derived composite double layer supercapacitors. *Carbon Trends* **2024**, *15*, 100359. https://doi.org/10.1016/j.cartre.2024.100359.
85. Manimekala, T.; Sivasubramanian, R.; Dar, M.A.; Dharmalingam, G. Crafting the architecture of biomass-derived activated carbon via electrochemical insights for supercapacitors: A review. *R. Soc. Chem.* **2025**, *15*, 2490–2522. https://doi.org/10.1039/d4ra07682f.
86. Inthawong, S.; Wongkoblap, A.; Intomya, W.; Tangsathitkulchai, C. The Enhancement of CO_2 and CH_4 Capture on Activated Carbon with Different Degrees of Burn-Off and Surface Chemistry. *Molecules* **2023**, *28*, 5433. https://doi.org/10.3390/molecules28145433.
87. Tahsin, M.; Shahinuzzaman, M.; Akter, T.; Abdur, R.; Bashar, M.S.; Kadir, M.R.; Hoque, S.; Jamal, M.S.; Hossain, M. Improved CO_2 adsorption and desorption using chemically derived activated carbon from corn cob hard shell. *Carbon Trends* **2025**, *19*, 100495. https://doi.org/10.1016/j.cartre.2025.100495.
88. Lee, S.Y.; Lee, J.H.; Kim, Y.H.; Rhee, K.Y.; Park, S.J. Roles of london dispersive and polar components of nano-metal-coated activated carbons for improving carbon dioxide uptake. *Coatings* **2021**, *11*, 691. https://doi.org/10.3390/coatings11060691.
89. Muzarpar, M.S.; Leman, A.M. The Adsorption Mechanism of Activated Carbon and Its Application-A Review. *Int. J. Adv. Technol. Mech. Mechatron. Mater.* **2021**, *1*, 118–124. https://doi.org/10.37869/ijatec.v1i3.37.
90. Lee, H.M.; Lee, B.H.; Park, S.J.; An, K.H.; Kim, B.J. Pitch-derived activated carbon fibers for emission control of low-concentration hydrocarbon. *Nanomaterials* **2019**, *9*, 1313. https://doi.org/10.3390/nano9091313.
91. Jepleting, A.; Mecha, A.C.; Sombei, D.; Moraa, D.; Chollom, M.N. Potential of low-cost materials for biogas purification, a review of recent developments. *Renew. Sustain. Energy Rev.* **2024**, *210*, 115152. https://doi.org/10.1016/j.rser.2024.115152.
92. Karimi, M.; Silva, J.A.C.; Gonçalves, C.N.D.P.; de Tuesta, J.L.D.; Rodrigues, A.E.; Gomes, H.T. CO_2 Capture in Chemically and Thermally Modified Activated Carbons Using Breakthrough Measurements: Experimental and Modeling Study. *Ind. Eng. Chem. Res.* **2018**, *57*, 11154–11166. https://doi.org/10.1021/acs.iecr.8b00953.
93. Osterrieth, J.W.M.; Rampersad, J.; Madden, D.; Rampal, N.; Skoric, L.; Connolly, B.; Allendorf, M.D.; Stavila, V.; Snider, J.L.; Ameloot, R.; et al. How Reproducible are Surface Areas Calculated from the BET Equation? *Adv. Mater.* **2022**, *34*, e2201502. https://doi.org/10.1002/adma.202201502.
94. Li, Y.; Liu, N.; Zhang, T.; Wang, B.; Wang, Y.; Wang, L.; Wei, J. Highly microporous nitrogen-doped carbons from anthracite for effective CO_2 capture and CO_2/CH_4 separation. *Energy* **2020**, *211*, 118561. https://doi.org/10.1016/j.energy.2020.118561.
95. Xing, L.A.; Yang, F.; Zhong, X.; Liu, Y.; Lu, H.; Guo, Z.; Lv, G.; Yang, J.; Yuan, A.; Pan, J. Ultra-microporous cotton fiber-derived activated carbon by a facile one-step chemical activation strategy for efficient CO2 adsorption. *Sep. Purif. Technol.* **2023**, *324*, 124470. https://doi.org/10.1016/j.seppur.2023.124470.
96. Ruiz, B.; Ferrera-Lorenzo, N.; Fuente, E. Valorisation of lignocellulosic wastes from the candied chestnut industry. Sustainable activated carbons for environmental applications. *J. Environ. Chem. Eng.* **2017**, *5*, 1504–1515. https://doi.org/10.1016/j.jece.2017.02.028.
97. Wei, H.; Deng, S.; Hu, B.; Chen, Z.; Wang, B.; Huang, J.; Yu, G. Granular Bamboo-Derived Activated Carbon for High CO_2 Adsorption: The Dominant Role of Narrow Micropores. *ChemSusChem* **2012**, *5*, 2354–2360. https://doi.org/10.1002/cssc.201200570.
98. Hong, S.M.; Jang, E.; Dysart, A.D.; Pol, V.G.; Lee, K.B. CO_2 capture in the sustainable wheat-derived activated microporous carbon compartments. *Sci. Rep.* **2016**, *6*, 34590. https://doi.org/10.1038/srep34590.
99. Cui, H.; Xu, J.; Shi, J.; You, S.; Zhang, C.; Yan, N.; Liu, Y.; Chen, G. Evaluation of different potassium salts as activators for hierarchically porous carbons and their applications in CO2 adsorption. *J. Colloid. Interface Sci.* **2021**, *583*, 40–49. https://doi.org/10.1016/j.jcis.2020.09.022.
100. Siemak, J.; Michalkiewicz, B. Adsorption Equilibrium of CO_2 on Microporous Activated Carbon Produced from Avocado Stone Using H2SO4 as an Activating Agent. *Sustainability* **2023**, *15*, 16881. https://doi.org/10.3390/su152416881.

101. Sahota, S.; Shah, G.; Ghosh, P.; Kapoor, R.; Sengupta, S.; Singh, P.; Vijay, V.; Sahay, A.; Vijay, V.K.; Thakur, I.S. Review of trends in biogas upgradation technologies and future perspectives. *Bioresour. Technol. Rep.* **2018**, *1*, 79–88. https://doi.org/10.1016/j.biteb.2018.01.002.
102. Choi, P.-S.; Jeong, J.-M.; Choi, Y.-K.; Kim, M.-S.; Shin, G.-J.; Park, S.-J. A review: Methane capture by nanoporous carbon materials for automobiles. *Carbon Lett.* **2016**, *17*, 18–28. https://doi.org/10.5714/CL.2016.17.1.018.
103. Liu, B.; Ma, X.; Wei, D.; Yang, Y.; Zeng, Z.; Li, L. Development of ultramicropore-mesopore interconnected pore architectures for boosting carbon dioxide capture at low partial pressure. *Carbon N. Y.* **2022**, *192*, 41–49. https://doi.org/10.1016/j.carbon.2022.02.028.
104. Serafin, J.; Narkiewicz, U.; Morawski, A.W.; Wróbel, R.J.; Michalkiewicz, B. Highly Microporous Activated Carbons from Biomass for CO2capture and Effective Micropores at Different Conditions. *J. CO_2 Util.* **2017**, *18*, 73–79. https://doi.org/10.1016/j.jcou.2017.01.006.
105. Peredo-Mancilla, D.; Hort, C.; Jeguirim, M.; Ghimbeu, C.M.; Limousy, L.; Bessieres, D. Experimental Determination of the CH_4 and CO_2 Pure Gas Adsorption Isotherms on Different Activated Carbons. *J. Chem. Eng. Data* **2018**, *63*, 3027–3034. https://doi.org/10.1021/acs.jced.8b00297.
106. Mehrmohammadi, P.; Ghaemi, A. Investigating the effect of textural properties on CO_2 adsorption in porous carbons via deep neural networks using various training algorithms. *Sci. Rep.* **2023**, *13*, 21264. https://doi.org/10.1038/s41598-023-48683-4.
107. Zhu, B.; Shang, C.; Guo, Z. Naturally Nitrogen and Calcium-Doped Nanoporous Carbon from Pine Cone with Superior CO_2 Capture Capacities. *ACS Sustain. Chem. Eng.* **2016**, *4*, 1050–1057. https://doi.org/10.1021/acssuschemeng.5b01113.
108. Choma, J.; Osuchowski, L.; Marszewski, M.; Dziura, A.; Jaroniec, M. Developing microporosity in Kevlar®-derived carbon fibers by CO_2activation for CO_2adsorption. *J. CO2 Util.* **2016**, *16*, 17–22. https://doi.org/10.1016/j.jcou.2016.05.004.
109. Sevilla, M.; Falco, C.; Titirici, M.-M.; Fuertes, A.B. High-performance CO_2 sorbents from algae. *RSC Adv.* **2012**, *2*, 12792–12797, https://doi.org/10.1039/c2ra22552b.
110. Minagawa, H.; Nishikawa, Y.; Ikeda, I.; Miyazaki, K.; Takahara, N.; Sakamoto, Y.; Komai, T.; Narita, H. Characterization of sand sediment by pore size distribution and permeability using proton nuclear magnetic resonance measurement. *J. Geophys. Res. Solid Earth* **2008**, *113*, B07210. https://doi.org/10.1029/2007JB005403.
111. Meng, M.; Ge, H.; Shen, Y.; Ji, W.; Li, Z. Insight into Water Occurrence and Pore Size Distribution by Nuclear Magnetic Resonance in Marine Shale Reservoirs, Southern China. *Energy Fuels* **2023**, *37*, 319–327. https://doi.org/10.1021/acs.energyfuels.2c03395.
112. Radlinski, A.P.; Mastalerz, M.; Hinde, A.L.; Hainbuchner, M.; Rauch, H.; Baron, M.; Lin, J.S.; Fan, L.; Thiyagarajan, P. Application of SAXS and SANS in evaluation of porosity, pore size distribution and surface area of coal. *Int. J. Coal Geol*. **2004**, *59*, 245–271. https://doi.org/10.1016/j.coal.2004.03.002.
113. Soto, C.; Cicuttin, N.; Carmona, F.J.; de la Viuda, M.; Tena, A.; Lozano, Á.E.; Hernández, A.; Palacio, L.; Prádanos, P. Gas adsorption isotherm, pore size distribution, and free volume fraction of polymer-polymer mixed matrix membranes before and after thermal rearrangement. *J. Memb. Sci.* **2023**, *683*, 121841. https://doi.org/10.1016/j.memsci.2023.121841.
114. Cornette, V.; Villarroel-Rocha, J.; Sapag, K.; Mons, R.D.; Toso, J.P.; López, R.H. Insensitivity in the pore size distribution of ultramicroporous carbon materials by CO_2 adsorption. *Carbon N. Y.* **2020**, *168*, 508–514. https://doi.org/10.1016/j.carbon.2020.07.011.
115. Shi, J.; Cui, H.; Xu, J.; Yan, N.; Zhang, C.; You, S. Fabrication of nitrogen doped and hierarchically porous carbon flowers for CO_2 adsorption. *J. CO_2 Util.* **2021**, *51*, 101617. https://doi.org/10.1016/j.jcou.2021.101617.
116. To, J.W.F.; He, J.; Mei, J.; Haghpanah, R.; Chen, Z.; Kurosawa, T.; Chen, S.; Bae, W.G.; Pan, L.; Tok, J.B.H.; Wilcox, J.; Bao, Z. Hierarchical N-Doped Carbon as CO_2 Adsorbent with High CO_2 Selectivity from Rationally Designed Polypyrrole Precursor. *J. Am. Chem. Soc.* **2016**, *138*, 1001–1009. https://doi.org/10.1021/jacs.5b11955.
117. Vieillard, J.; Bouazizi, N.; Bargougui, R.; Brun, N.; Fotsing Nkuigue, P.; Oliviero, E.; Thoumire, O.; Couvrat, N.; Djoufac Woumfo, E.; Ladam, G.; Mofaddel, N.; Azzouz, A.; Le Derf, F. Cocoa shell-deriving hydrochar modified through aminosilane grafting and cobalt particle dispersion as potential carbon dioxide adsorbent. *Chem. Eng. J.* **2018**, *342*, 420–428. https://doi.org/10.1016/j.cej.2018.02.084.
118. Stevens, R.W.; Siriwardane, R.V.; Logan, J. In situ fourier transform infrared (FTIR) investigation of CO_2 adsorption onto zeolite materials. *Energy Fuels* **2008**, *22*, 3070–3079. https://doi.org/10.1021/ef800209a.
119. Ghouma, I.; Jeguirim, M.; Dorge, S.; Limousy, L.; Ghimbeu, C.M.; Ouederni, A. Activated carbon prepared by physical activation of olive stones for the removal of NO_2 at ambient temperature. *Comptes Rendus Chim.* **2015**, *18*, 63–74. https://doi.org/10.1016/j.crci.2014.05.006.

120. Staudt, J.; Musial, C.M.; Canevesi, R.; Fierro, V.; Ribeiro, C.; Alves, H.J.; Borba, C.E. Evaluation of the CH_4/CO_2 Separation by Adsorption on Coconut Shell Activated Carbon: Impact of the Gas Moisture on Equilibrium Selectivity and Adsorption Capacity. *Heliyon* **2024**, *10*, e30368. https://doi.org/10.1016/j.heliyon.2024.e30368.
121. Kamgang Maffo, E.; Clementine-Christelle, M.-E.; Kombou, V. Production of Activated Carbons: Processes, Applications, and Environmental Considerations. 2024. Available online: https://papers.ssrn.com/sol3/papers.cfm?abstract_id=5025307 (accessed on 1 April 2025). https://doi.org/10.2139/ssrn.5025307.
122. Plaza, M.G.; Pevida, C.; Martín, C.F.; Fermoso, J.; Pis, J.J.; Rubiera, F. Developing almond shell-derived activated carbons as CO_2 adsorbents. *Sep. Purif. Technol.* **2010**, *71*, 102–106. https://doi.org/10.1016/j.seppur.2009.11.008.
123. Álvarez-Gutiérrez, N.; Gil, M.V.; Rubiera, F.; Pevida, C. Adsorption Performance Indicators for the CO2/CH4 Separation: Application to Biomass-Based Activated Carbons. *Fuel Process. Technol.* **2016**, *142*, 361–369. https://doi.org/10.1016/j.fuproc.2015.10.038.
124. Peredo-Mancilla, D.; Ghouma, I.; Hort, C.; Ghimbeu, C.M.; Jeguirim, M.; Bessieres, D. CO_2 and CH_2 adsorption behavior of biomass-based activated carbons. *Energies* **2018**, *11*, 3136. https://doi.org/10.3390/en11113136.
125. Ferrera-Lorenzo, N.; Fuente, E.; Suárez-Ruiz, I.; Ruiz, B. Sustainable activated carbons of macroalgae waste from the Agar-Agar industry. Prospects as adsorbent for gas storage at high pressures. *Chem. Eng. J.* **2014**, *250*, 128–136. https://doi.org/10.1016/j.cej.2014.03.119.
126. Ogungbenro, A.E.; Quang, D.V.; Al-Ali, K.A.; Vega, L.F.; Abu-Zahra, M.R.M. Physical synthesis and characterization of activated carbon from date seeds for CO_2 capture. *J. Environ. Chem. Eng.* **2018**, *6*, 4245–4252. https://doi.org/10.1016/j.jece.2018.06.030.
127. Vilella, P.C.; Lira, J.A.; Azevedo, D.C.S.; Bastos-Neto, M.; Stefanutti, R. Preparation of biomass-based activated carbons and their evaluation for biogas upgrading purposes. *Ind. Crops Prod*. **2017**, *109*, 134–140. https://doi.org/10.1016/j.indcrop.2017.08.017.
128. Deng, S.; Hu, B.; Chen, T.; Wang, B.; Huang, J.; Wang, Y.; Yu, G. Activated carbons prepared from peanut shell and sunflower seed shell for high CO_2 adsorption. *Adsorption* **2015**, *21*, 125–133. https://doi.org/10.1007/s10450-015-9655-y.
129. Mopoung, S.; Dejang, N. Activated Carbon Preparation from Eucalyptus Wood Chips using Continuous Carbonization-Steam Activation Process in a Batch Intermittent Rotary Kiln. *Sci. Rep.* **2020**, *11*, 13948. https://doi.org/10.21203/rs.3.rs-128184/v1.
130. Bedia, J.; Peñas-Garzón, M.; Gómez-Avilés, A.; Rodriguez, J.J.; Belver, C. Review on Activated Carbons by Chemical Activation with $FeCl_3$. *C* **2020**, *6*, 21. https://doi.org/10.3390/c6020021.
131. Wang, J.; Kaskel, S. KOH activation of carbon-based materials for energy storage. *J. Mater. Chem.* **2012**, *22*, 23710–23725. https://doi.org/10.1039/c2jm34066f.
132. Serafin, J.; Dziejarski, B.; Sreńscek-Nazzal, J. An innovative and environmentally friendly bioorganic synthesis of activated carbon based on olive stones and its potential application for CO_2 capture. *Sustain. Mater. Technol.* **2023**, *38*, e00717. https://doi.org/10.1016/j.susmat.2023.e00717.
133. Saadi, W.; Rodríguez-Sánchez, S.; Ruiz, B.; Najar-Souissi, S.; Ouederni, A.; Fuente, E. From pomegranate peels waste to one-step alkaline carbonate activated carbons. Prospect as sustainable adsorbent for the renewable energy production. *J. Environ. Chem. Eng.* **2022**, *10*, 107010. https://doi.org/10.1016/j.jece.2021.107010.
134. Prauchner, M.J.; Oliveira, S.d.C.; Rodríguez-Reinoso, F. Tailoring Low-Cost Granular Activated Carbons Intended for CO_2 Adsorption. *Front. Chem.* **2020**, *8*, 581133. https://doi.org/10.3389/fchem.2020.581133.
135. Plaza, M.G.; González, A.S.; Pis, J.J.; Rubiera, F.; Pevida, C. Production of Microporous Biochars by Single-Step Oxidation: Effect of Activation Conditions on CO_2 Capture. *Appl. Energy* **2014**, *114*, 551–562. https://doi.org/10.1016/j.apenergy.2013.09.058.
136. Krupšová, S.; Almáši, M. Cellulose–Amine Porous Materials: The Effect of Activation Method on Structure, Textural Properties, CO_2 Capture, and Recyclability. *Molecules* **2024**, *29*, 1158. https://doi.org/10.3390/molecules29051158.
137. Álvarez-Gutiérrez, N.; García, S.; Gil, M.V.; Rubiera, F.; Pevida, C. Dynamic Performance of Biomass-Based Carbons for CO_2/CH_4 Separation. Approximation to a Pressure Swing Adsorption Process for Biogas Upgrading. *Energy Fuels* **2016**, *30*, 5005–5015. https://doi.org/10.1021/acs.energyfuels.6b00664.
138. Guo, Y.; Tan, C.; Sun, J.; Li, W.; Zhang, J.; Zhao, C. Porous activated carbons derived from waste sugarcane bagasse for CO_2 adsorption. *Chem. Eng. J.* **2020**, *381*, 122736. https://doi.org/10.1016/j.cej.2019.122736.
139. Arami-Niya, A.; Daud, W.M.A.W.; Mjalli, F.S. Comparative study of the textural characteristics of oil palm shell activated carbon produced by chemical and physical activation for methane adsorption. *Chem. Eng. Res. Des.* **2011**, *89*, 657–664. https://doi.org/10.1016/j.cherd.2010.10.003.

140. Serafin, J.; Dziejarski, B.; Fonseca-Bermúdez, Ó.J.; Giraldo, L.; Sierra-Ramírez, R.; Bonillo, M.G.; Farid, G.; Moreno-Piraján, J.C. Bioorganic Activated Carbon from Cashew Nut Shells for H_2 Adsorption and H_2/CO_2, H_2/CH_4, CO_2/CH_4, $H_2/CO_2/CH_4$ Selectivity in Industrial Applications. *Int. J. Hydrogen Energy* **2024**, *86*, 662–676. https://doi.org/10.1016/j.ijhydene.2024.08.417.
141. Sreńscek-Nazzal, J.; Kiełbasa, K. Advances in modification of commercial activated carbon for enhancement of CO_2 capture. *Appl. Surf. Sci.* **2019**, *494*, 137–151. https://doi.org/10.1016/j.apsusc.2019.07.108.
142. Phalakornkule, C.; Foungchuen, J.; Pitakchon, T. Impregnation of Chitosan onto Activated Carbon for High Adsorption Selectivity towards CO_2 : CO_2 Capture from Biohydrogen, Biogas and Flue Gas. *J. Sustain. Energy Environ.* **2012**, *3*, 153–157.
143. Rattanaphan, S.; Rungrotmongkol, T.; Kongsune, P. Biogas improving by adsorption of CO_2 on modified waste tea activated carbon. *Renew. Energy* **2020**, *145*, 622–631. https://doi.org/10.1016/j.renene.2019.05.104.
144. Reljic, S.; Martinez-Escandell, M.; Silvestre-Albero, J. Effect of Porosity and Surface Chemistry on CO_2 and CH_4 Adsorption in S-Doped and S-/O-co-Doped Porous Carbons. *C-J. Carbon Res.* **2022**, *8*, 41. https://doi.org/10.3390/c8030041.
145. Peredo-Mancilla, D.; Ghimbeu, C.M.; Réty, B.; Ho, B.N.; Pino, D.; Vaulot, C.; Hort, C.; Bessieres, D. Surface-Modified Activated Carbon with a Superior CH4/CO2Adsorption Selectivity for the Biogas Upgrading Process. *Ind. Eng. Chem. Res.* **2022**, *61*, 12710–12727. https://doi.org/10.1021/acs.iecr.2c01264.
146. Domínguez-Ramos, L.; Prieto-Estalrich, A.; Malucelli, G.; Gómez-Díaz, D.; Freire, M.S.; Lazzari, M.; González-álvarez, J. N-and S-Doped Carbons Derived from Polyacrylonitrile for Gases Separation. *Sustainability* **2022**, *14*, 3760. https://doi.org/10.3390/su14073760.
147. Jang, D.-I.; Park, S.-J. Influence of nickel oxide on carbon dioxide adsorption behaviors of activated carbons. *Fuel* **2012**, *102*, 439–444. https://doi.org/10.1016/j.fuel.2012.03.052.
148. Lu, X.; Jin, D.; Wei, S.; Zhang, M.; Zhu, Q.; Shi, X.; Deng, Z.; Guo, W.; Shen, W. Competitive adsorption of a binary CO_2-CH_4 mixture in nanoporous carbons: Effects of edge-functionalization. *Nanoscale* **2015**, *7*, 1002–1012. https://doi.org/10.1039/c4nr05128a.
149. Hedin, N.; Andersson, L.; Bergström, L.; Yan, J. Adsorbents for the post-combustion capture of CO_2 using rapid temperature swing or vacuum swing adsorption. *Appl. Energy* **2013**, *104*, 418–433. https://doi.org/10.1016/j.apenergy.2012.11.034.
150. Aguilar-Armenta, G.; Patiño-Iglesias, M.E.; Leyva-Ramos, R. Adsorption Kinetic Behaviour of Pure CO_2, N_2 and CH_4 in Natural Clinoptilolite at Different Temperatures. *Adsorpt. Sci. Technol.* **2003**, *21*, 81–91. https://doi.org/10.1260/02636170360699831.
151. Yu, H.-R.; Cho, S.; Bai, B.C.; Yi, K.B.; Lee, Y.-S. Effects of fluorination on carbon molecular sieves for CH_4/CO_2 gas separation behavior. *Int. J. Greenh. Gas Control* **2012**, *10*, 278–284. https://doi.org/10.1016/j.ijggc.2012.06.013.
152. Punpee, S.; Tongpadungrod, P.; Suttikul, T.; Phalakornkule, C. Characteristics of CO_2 adsorption and desorption on activated carbon in comparison with zeolite 13X and carbon molecular sieve and applications in biogas upgrading using vacuum pressure swing adsorption. *J. Chem. Technol. Biotechnol.* **2023**, *98*, 2677–2690. https://doi.org/10.1002/jctb.7320.
153. Rainone, F.; D'Agostino, O.; Erto, A.; Balsamo, M.; Lancia, A. Biogas upgrading by adsorption onto activated carbon and carbon molecular sieves: Experimental and modelling study in binary CO_2/CH_4 mixture. *J. Environ. Chem. Eng.* **2021**, *9*, 106256. https://doi.org/10.1016/j.jece.2021.106256.
154. Gil, M.V.; Álvarez-Gutiérrez, N.; Martínez, M.; Rubiera, F.; Pevida, C.; Morán, A. Carbon adsorbents for CO_2 capture from bio-hydrogen and biogas streams: Breakthrough adsorption study. *Chem. Eng. J.* **2015**, *269*, 148–158. https://doi.org/10.1016/j.cej.2015.01.100.
155. Rios, R.B.; Stragliotto, F.M.; Peixoto, H.R.; Torres, A.E.B.; Bastos-Neto, M.; Azevedo, D.C.S.; Cavalcante Jr, C.L Studies on the adsorption behavior of CO_2-CH_4 mixtures using activated carbon. *Braz. J. Chem. Eng.* **2013**, *30*, 939–951. https://doi.org/10.1590/S0104-66322013000400024.
156. Zhang, B.; Liu, P.; Huang, Z.; Liu, J. Adsorption Equilibrium and Diffusion of CH_4, CO_2, and N_2 in Coal-Based Activated Carbon. *ACS Omega* **2023**, *8*, 10303–10313. https://doi.org/10.1021/acsomega.2c07910.
157. Chinea, L.; Slopiecka, K.; Bartocci, P.; Alissa Park, A.-H.; Wang, S.; Jiang, D.; Fantozzi, F. Methane enrichment of biogas using carbon capture materials. *Fuel* **2023**, *334*, 126428. https://doi.org/10.1016/j.fuel.2022.126428.
158. Bacsik, Z.; Cheung, O.; Vasiliev, P.; Hedin, N. Selective separation of CO_2 and CH_4 for biogas upgrading on zeolite NaKA and SAPO-56. *Appl. Energy* **2016**, *162*, 613–621. https://doi.org/10.1016/j.apenergy.2015.10.109.
159. Saha, D.; Bao, Z.; Jia, F.; Deng, S. Adsorption of CO_2, CH_4, N_2O, and N_2 on MOF-5; MOF-177, and zeolite 5A. *Environ. Sci. Technol.* **2010**, *44*, 1820–1826. https://doi.org/10.1021/es9032309.
160. Peredo-Mancilla, D.; Ghimbeu, C.M.; Ho, B.N.; Jeguirim, M.; Hort, C.; Bessieres, D. Comparative study of the CH_4/CO_2 adsorption selectivity of activated carbons for biogas upgrading. *J. Environ. Chem. Eng.* **2019**, *7*, 103368. https://doi.org/10.1016/j.jece.2019.103368.

161. Dreisbach, F.; Staudt, R.; Keller, J.U. High pressure adsorption data of methane, nitrogen, carbon dioxide and their binary and ternary mixtures on activated carbon. *Adsorption* **1999**, *5*, 215–227. https://doi.org/10.1023/A:1008914703884.
162. Zaidi, S.T.H.; Ahmad, A.; Ismail, M.; Nordin, N.A.H.M.; Bustam, M.A.; Usman, M.; Asubonteng, D.; ul Hasnain, S.M.W. Enhanced CO_2 adsorption and selectivity in CNT and piperazine modified Ni-MOF-74 nanocomposites. *Solid State Sci.* **2025**, *161*, 107855. https://doi.org/10.1016/j.solidstatesciences.2025.107855.
163. Amasha, H.; Ahmad, A.; Abdulazeez, I.; Al Hamouz, O.C.S. Microwave-synthesized heteroaromatic porous organic polymers for CO2 capture and hydrogen storage. *Mater. Today Sustain.* **2024**, *27*, 100879. https://doi.org/10.1016/j.mtsust.2024.100879.
164. Bentivoglio, D.; Chiaraluce, G.; Finco, A. Economic assessment for vegetable waste valorization through the biogas-biomethane chain in Italy with a circular economy approach. *Front. Sustain. Food Syst.* **2022**, *6*, 1035357. https://doi.org/10.3389/fsufs.2022.1035357.
165. Rusanowska, P.; Zieliński, M.; Dębowski, M. Removal of CO_2 from Biogas during Mineral Carbonation with Waste Materials. *Int. J. Environ. Res. Public Health* **2023**, *20*, 5687. https://doi.org/10.3390/ijerph20095687.
166. Baldinelli, A.; Desideri, U.; Fantozzi, F.; Cinti, G. Biogas-to-Power Systems Based on Solid Oxide Fuel Cells: Thermodynamic Analysis of Stack Integration Strategies. *Energies* **2024**, *17*, 3614. https://doi.org/10.3390/en17153614.